HMJ Corporation

10400 CONNECTICUT AVENUE, SUITE 404
KENSINGTON, MARYLAND 20895-3910

REPORT NO. 92-HMJ-117

DISK MHD CONVERSION SYSTEM FOR NERVA REACTOR

W. D. Jackson, Editor

January 13, 1992

RESEARCH SUPPORTED BY THE STRATEGIC DEFENSE INITIATIVE/INNOVATIVE SCIENCE AND TECHNOLOGY AND MANAGED BY THE DEPARTMENT OF ENERGY, IDAHO OPERATIONS OFFICE UNDER CONTRACT NO. DE-AC07-91ID19925

Accession Number: 4388

Publication Date: Jan 13, 1992

Title: Disk MHD Conversion System for Nerva Reactor

Personal Author: Jackson, W.D. (Editor)

Corporate Author Or Publisher: HMJ Corp., 10400 Connecticut Ave., Kensington, MD 20895-3910
Report Number: 92-HMJ-117

Descriptors, Keywords: Disk MHD Conversion NERVA Reactor Space Power

Pages: 00068

Cataloged Date: Mar 18, 1993

Contract Number: DE-AC07-91ID19925

Document Type: HC

Number of Copies In Library: 000001

Record ID: 26465

SUMMARY

The combination of a magnetohydrodynamic (MHD) generator of the disk type with a NERVA reactor yields an advanced space power system with the capability of producing up to gigawatt pulses and multi-megawatt continuous operating capability. Cesium seeding is utilized in the disk generator under conditions which enable it to operate stably in the non-equilibrium electrical conduction mode. Several unique features result from the combination of this type of reactor and a disk MHD generator in which hydrogen serves as the plasma working fluid. In common with all practical MHD generators, the disk output is DC and voltages in the range 20-100kV are attainable. This leads to a simplification of the power conditioning system and a major reduction in its specific mass. Taken together with the high performance capabilities of the NERVA reactor, the result is an attractively low overall system specific mass. Further, the use of non-equilibrium ionization yields high system enthalpy extractions, values in excess of 40% being attainable.

The development of the basis for the design of a cesium seeded hydrogen MHD disk generator was the objective of the study covered by this report. The detailed design, construction and testing of this generator will constitute the next phase of the work. The report begins with a discussion of the issues and establishes a reference case in which the required enthalpy extraction is obtained for output voltages in the region of 40 kV. Recognizing that considerable experience has been obtained with cesium seeded noble gases (principally argon and helium) in non-equilibrium MHD generators, but that this is not the case for hydrogen, a detailed account of the plasma modeling undertaken is given. This is used to determine generator performance in terms of parameters such as energy loss factor and to establish the regions of stable and unstable flows. The experimental conditions required for the clarification of the plasma behavior are next identified and the preliminary design of the required facilities is presented. A discussion of directions which should be taken in later phases of the project is also included.

The principal results of the study have been to: 1) confirm that cesium-seeded hydrogen plasma disk MHD generator can meet its expected performance while operating in a stable plasma regime; and 2) identify the conditions under which plasma properties and generator performance can be experimentally established. The next phase of the project will involve the design, construction and testing of a sub-scale model of this type of generator. The results of this work will be scalable to the design of a prototype system, either as a space power supply or in a combined power supply/thruster configuration. The goal of the project is to demonstrate that attractively low specific mass space power systems are achievable with this technology for multi-megawatt power level applications. It will also contribute to the development of the disk generator for terrestrial MHD systems, particularly in central station electric utility applications.

DISK MHD CONVERSION SYSTEM FOR NERVA REACTOR

W. D. Jackson, Editor

Contributing Authors

F. E. Bernard
S. T. Demetriades
R. Holman
W. D. Jackson
C. D. Maxwell
G. R. Seikel

HMJ CORPORATION

Research supported by
Strategic Defense Initiative/Innovative Science and Technology
and managed by
Department of Energy, Idaho Operations Office

January 13, 1992

DEDICATION

This report is dedicated to the memory of Professor Jean Louis who was a pioneering advocate of non-equilibrium MHD disk generators operating on cesium seeded hydrogen from a NERVA nuclear heat source. His extensive work on both system and plasma aspects inspired this project and provided a most valuable starting point from which to develop the results herein reported.

PREFACE

As the development of space proceeds, electrical power requirements will surely increase. It is already a straightforward matter to project requirements into the megawatt range. Two major candidates can be discerned, the first involving a steady supply of multi-megawatt electric power and the second, power pulses extended into the level of hundreds of megawatts for the period measured in seconds.

In terrestrial electric systems, the handling of electric power at the gigawatt level is routine and the technologies involved are of a mature character. The space power system environment, however, does not permit the direct utilization of large scale terrestrial electric technologies, primarily because the specific mass of these is orders of magnitude removed from that acceptable for transport from the surface of the earth.

As a practical matter, multi-megawatt systems have limited primary energy sources available, amongst which a nuclear reactor is the outstanding candidate. Further, for the thermal to electric conversion step, what are frequently referred to as unconventional systems are promising candidates. The development of one of these, magnetohydrodynamic (MHD) power generation, for terrestrial application has been under way now for nearly three decades, but early schemes involving nuclear reactors were not pursued because of the low temperatures in these heat sources. On the other hand, the need for a nuclear propulsion system was recognized and the development of the NERVA type of reactor resulted not only in a demonstration of a successful propulsion system, but also a source suitable for an MHD generator of high performance. The potential of such a system was recognized by the late Professor Jean Louis to whom this report is dedicated.

The steps which led to the work reported here being possible were: first, recognition that alkali seeded hydrogen could achieve non-equilibrium ionization as in noble gases such as argon and helium for which considerable experience has been gained; second, that very low seed fractions leading to complete ionization were necessary to achieve stable non-equilibrium conditions; and third, that the high voltage characteristics on the MHD disk generator enabled power conditioning of acceptable specific mass to be utilized.

Based on these considerations and utilizing the results of a multi-megawatt space power system study conducted by Westinghouse Corporation, the HMJ Corporation established a team to determine the required operating conditions for a disk MHD conversion system driven by a NERVA reactor and to undertake an engineering demonstration of a generator of this type. The team comprises of C. R. Maxwell and S. T. Demetriades from the STD Research Corporation, G. R. Seikel, from SeiTec, Inc., F. E. Bernard from Westinghouse Corporation, and R. Holman, a HMJ Consultant who was heavily involved in the original NERVA reactor design, construction and testing, as well as in the Westinghouse system study. The system analysis work was undertaken by F. E.

Bernard, R. Holman, and G. R. Seikel. Plasma modeling and experiment design were contributed by C. D. Maxwell, with the HMJ Corporation participating in both system analysis and power conditioning design. Project review was undertaken by S. T. Demetriades and G. R. Seikel. The technical contributions of these team members are gratefully acknowledged as are the efforts of the editorial and word processing staffs of the HMJ Corporation, STD Research Corporation and Business Assistants to produce this report.

DISK MHD CONVERSION SYSTEMS FOR NERVA REACTOR

TABLE OF CONTENTS

TABLE OF CONTENTS (Continued)

LIST OF FIGURES

LIST OF FIGURES (Continued)

LIST OF TABLES

NOMENCLATURE

Roman Letters

a	=	Nonuniformity Parameter; $a = \left(\frac{1-\langle\alpha\rangle}{\langle\alpha\rangle}\right)^2$ for $\langle\alpha\rangle > 0.5$ and $a = 1$ for $\langle\alpha\rangle < 0.5$
B	=	Magnitude of Magnetic Induction
$\vec{B}$	=	Magnetic Induction Vector
E	=	Magnitude of Electric Field
$\vec{E}$	=	Electric Field in Laboratory Frame
$\vec{E}'$	=	Electric Field in Moving Frame; $\vec{E}' = \vec{E} + \vec{U} \times \vec{B}$
g_i	=	Internal Partition Functions for the Seed Ion in the Saha Equation
g_n	=	Internal Partition Functions for the Neutral Species in the Saha Equation
h	=	Planck's Constant
J	=	Magnitude of Current Density
$\vec{J}$	=	Current Density Vector
k	=	Boltzmann Constant
K	=	Load Factor. For the Disk Generator $K \equiv \frac{J_r}{J_{r,E_r=0}}$
L	=	Inductance
m	=	Particle Mass
P	=	Power
$\hat{P}$	=	Power Density
n	=	Number Density
p	=	Pressure
Q	=	Collision Cross Section
r	=	Radius
t	=	Time
T	=	Temperature
U	=	Magnitude of Mean Velocity
$\vec{U}$	=	Velocity Vector
V	=	Volume

NOMENCLATURE (Continued)

Greek Letters

$\langle\alpha\rangle$	=	Degree of Ionization
β	=	Hall Parameter
γ	=	Ratio of Specific Heats = c_p/c_v
δ_{eff}	=	Effective Electron Energy Loss Factor
δ'	=	Inelastic Electron Energy Loss Factor: $\delta_{\text{eff}} = \delta'(2m_e/m_a)$
η	=	Efficiency
μ	=	Magnetic Permeability
ν	=	Viscosity, Collision Frequency
ρ	=	Density
σ	=	Electrical Conductivity; Stefan-Boltzmann constant
τ	=	Time Constant

Subscripts

0	=	Initial Conditions; Combustor Conditions
1	=	Channel Inlet Conditions
2	=	Channel Exit Conditions
a	=	Heavy Particles
e	=	Electric; Electron
o	=	Stagnation Conditions; Vacuum Conditions
p	=	With Respect to Pressure
r	=	Radial Direction
t	=	Throat Conditions; Total
u	=	With Respect to Velocity
v	=	With Respect to Volume; Vibrational
κ	=	Component Species
θ	=	Azimuthal Direction

CHAPTER 1

INTRODUCTION, OBJECTIVES AND SYSTEM DESCRIPTION

1.1 Introduction

The wide range of electric power supply requirements for SDIO missions is well recognized to include (a) hundreds of MW of power for pulse applications, (b) high kW to low MW power levels for propulsion; and (c) up to several hundred kilowatts for on-board systems. Amongst the several primary energy sources being considered, the high temperature gas-cooled reactor of the NERVA type is attractive for both pulse power and electric propulsion applications. Indeed, it is especially significant in that it offers the possibility of meeting these two requirements with a single reactor in a power reactor in a power system with specific low mass and high enthalpy extraction characteristics not possible with competing sources.

This report presents the results obtained in a preliminary study of a magnetohydrodynamic (MHD) energy conversion system compatible with this reactor and offering an advanced system with attractively low specific mass (kg/kW), high specific enthalpy extraction and dual mode operation. The particular MHD converter is the non-equilibrium generator with disk geometry. For terrestrial applications, non-equilibrium MHD generators have been proposed and investigated to a limited extent using cesium seeded noble gases, helium or argon, as the working fluid but it was pointed out by the late Professor Louis that non-equilibrium ionization could also exist in hydrogen, which is the preferred working fluid for a NERVA type reactor.*

Within the resources available for an SBIR project, it is evidently not possible to undertake the complete development of a conversion system of the type discussed here. Rather, it is appropriate to identify the critical engineering issues and to determine how they may be realistically addressed and resolved. It is the intent of the project on which this report is based to meet this goal.

To ensure that the nuclear system, and MHD plasma aspects were adequately covered, it was necessary to assemble a team with the requisite expertise and resources. To meet this requirement, the HMJ Corporation (HMJ) has teamed with STD Research Corporation (STD) and the Westinghouse Electric Corporation, Advanced Energy Systems Department (W-AESD) and SeiTec to obtain the necessary MHD and nuclear expertise respectively. This team has the needed resources and the familiarity with the critical engineering issues

*References are listed following Chapter 7.

to provide SDIO with a design basis for a multi-megawatt NERVA-MHD disk space electric power system. The design itself would be undertaken as a follow on (Phase III) effort.

As explained in the following sections, the project strategy in Phase I was to identify the disk MHD generator operating conditions as they are dictated by system requirements and to address the fundamental aspects of non-equilibrium ionization in cesium seeded hydrogen. In the major second phase (Phase II), detailed system studies to determine system performance in both pulsed and continuous operating modes and experimental studies on a non-equilibrium disk MHD generator operating at appropriate conditions are intended to be the major project activities.

1.2 Objectives

The specific objectives identified at the outset of the work reported here were as follows:

1. Definition of the overall system in sufficient detail to establish the required conditions in the MHD generator channel, including both high power (up to 1GW) short time operation and sustained megawatts of power.

2. Model a cesium seeded hydrogen plasma in sufficient detail to enable its behavior to be established.

3. Develop requirements for experiments to investigate non-equilibrium phenomena in hydrogen at temperatures typical of NERVA systems.

4. Define and design credible engineering experiments suitable for an investigation of seeded hydrogen non-equilibrium plasma characteristics in an MHD disk generator and the performance of the generator itself.

The results obtained are presented successively in Chapters 2 through 5 and recommendations for further work in Phase II are given in Chapter 6.

1.3 System Description

Missions identified by the Space Defense Initiative Organization (SDIO) have included (1) electric power supply requirements in the range of 100s of MW for pulse applications; (2) high kW to low MW levels for electric propulsion; and (3) up to several hundred kilowatts for onboard systems, the so-called house-keeping load. The NERVA type of high temperature gas cooled reactor (Ref. 1), originally developed as a propulsion system, is directly applicable as a heat source for electric power generation for both pulse power and electric propulsion applications and can also service the house-keeping load.

Two basic modes of system operation are possible, depending on the type of mission, are shown in Figure 1. Figure 1a shows a system dedicated to electric power generation and having zero thrust, a condition easily realized with the disk geometry of the magnetohydrodynamic (MHD) energy conversion system considered in this study. A combined propulsion-electric generation system is shown in Figure 1b and is attractive for inter-orbital transfers and missions to the planets. In both cases, it is important to note that this system meets both generation and propulsion requirements with a single reactor in a power system which the Phase I study has confirmed to have low mass and high enthalpy extraction, characteristics not possible with competing MHD sources.

The system specifically considered in Phase I is depicted in Figure 1a. Hydrogen flow sequentially cools the power conditioning system, disk generator and magnet system and reactor structure before entering the reactor core for final heating to 2900K. This provides very advantageous recuperative approach which not only provides for cryogenic operating conditions where these are desired but also avoids the need for a heat rejection system, thus minimizing the thermal input required from the reactor.

The cesium seed required by the MHD generator is introduced after cooling and before entering the reactor to ensure thorough mixing. This is possible with the small amount of seed required but seed injection could also take place after the reactor, provided adequate mixing occurs.

As discussed and justified in later Chapters, the stability of the plasma working fluid with respect to electrical conductivity is ensured by limiting the cesium seeding level to the order of 1.5×10^{-5} molar concentration. This also ensures that this conductivity is not a function of the temperature of the gas entering the generator by virtue of full ionization.

The importance of achieving low seed fractions was established by the MHD group at the Tokyo Institute of Technology, working in cooperation with the late Professor Louis, and has been demonstrated with argon and helium in experimental work conducted by that organization. This Tokyo MHD group will be involved in the next phase of the project as indicated in Chapters 4 and 6. It was also pointed out by Louis that non-equilibrium ionization in hydrogen could be utilized in MHD generators. However, no corresponding data or experience are available for this gas, which is the preferred fluid for the NERVA reactor.

Accordingly, the technical effort in Phase I was devoted to establish that (1) stable non-equilibrium ionization can be obtained in a cesium seeded hydrogen plasma under conditions which would confirm the attractive system characteristics of the NERVA-disk MHD generator system; and (2) the energy input required to maintain the electrons at their elevated temperature is acceptable. As the immediately following Chapters will show, the existence of a favorable operating regime has been conclusively established and the basis for proceeding to a Phase II experimental demonstration of operation has been successfully created.

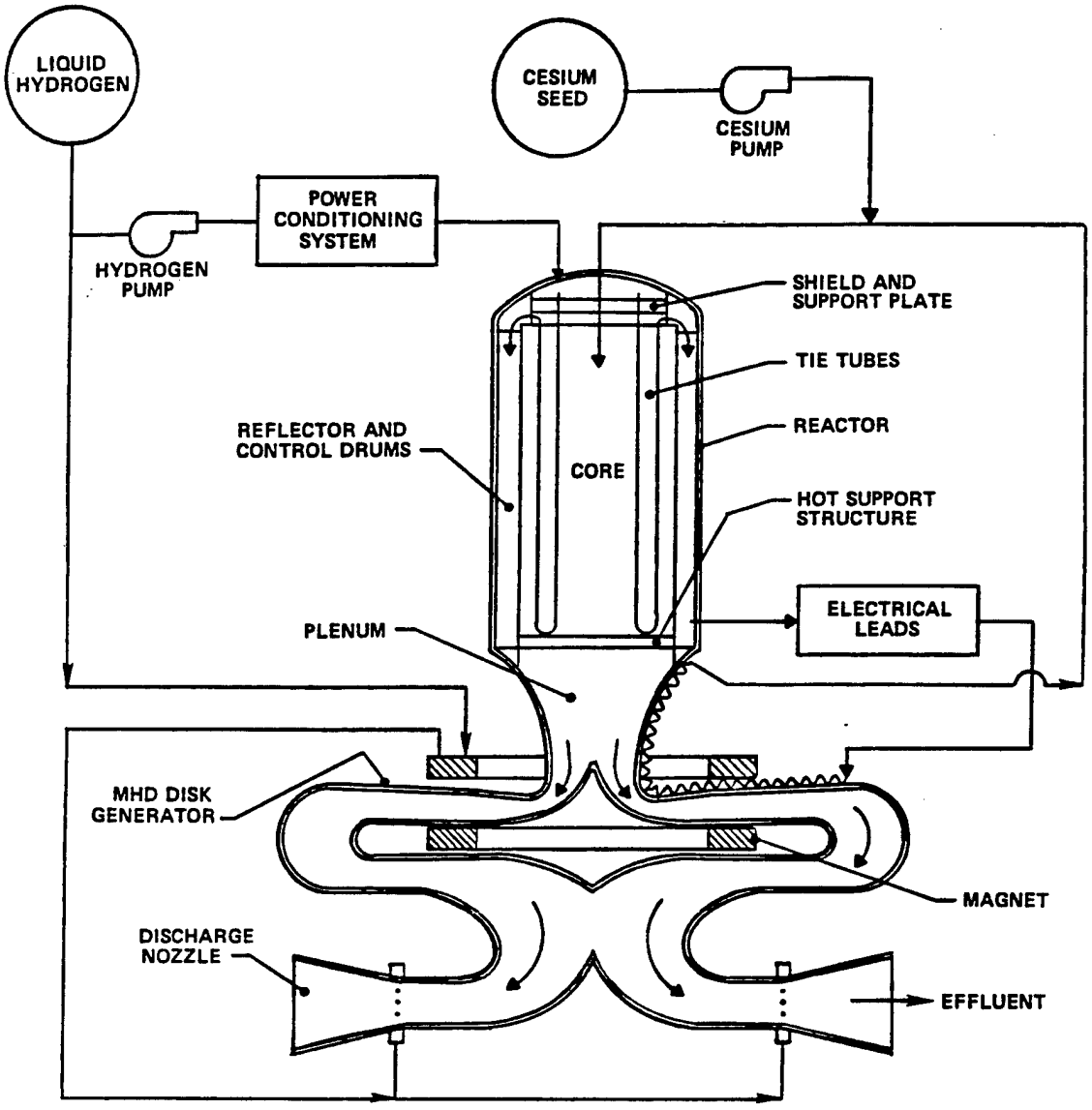

Fig. 1. (a) Radial Discharge - Neutralized Thrust
NERVA-MHD Disk Generator Space Power System.

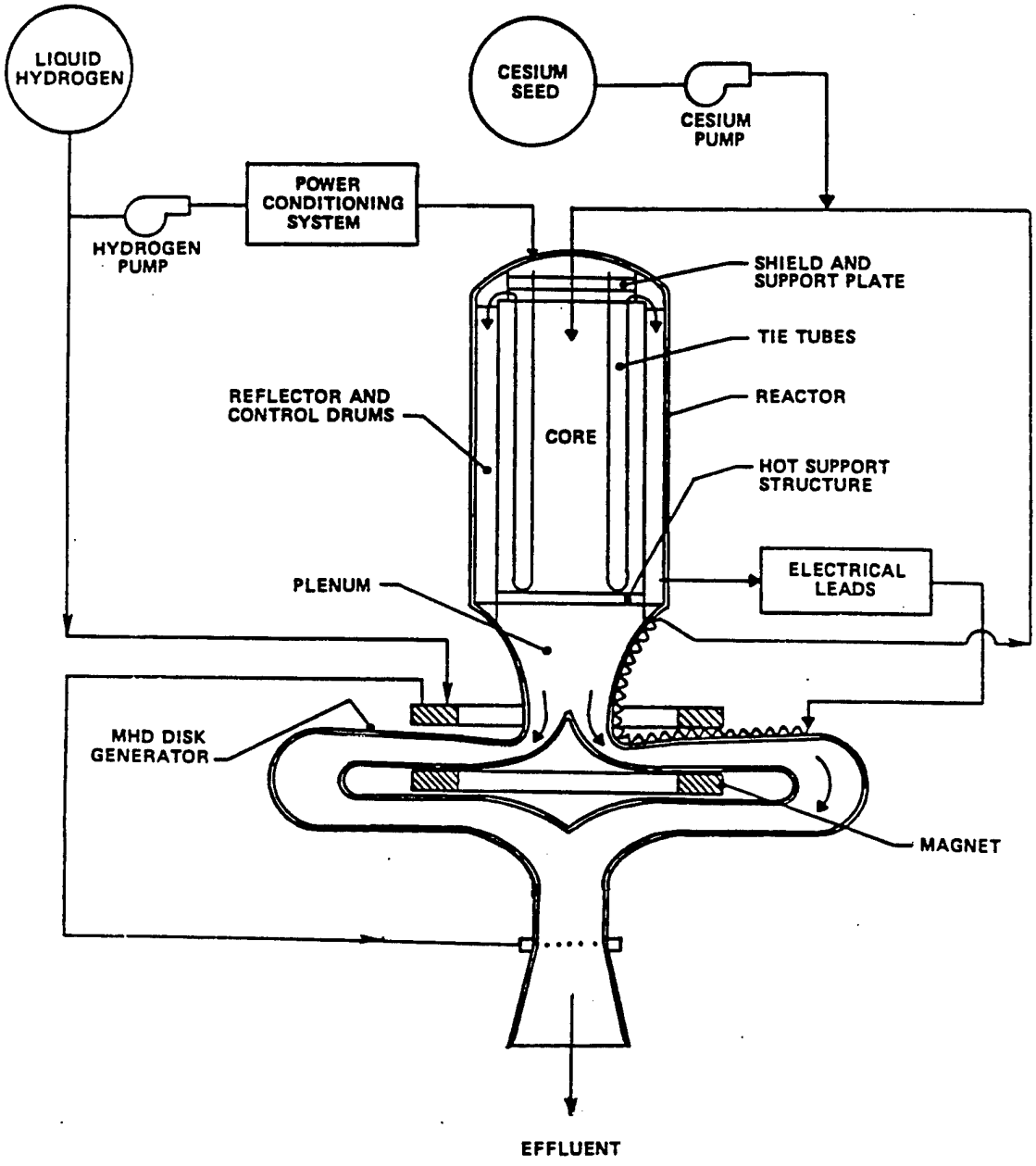

Fig. 1. (b) Axial Discharge - Thrust Mode.
NERVA-MHD Disk Generator Space Power System.

The low levels of cesium seeding required also minimize the mass of the working fluid and this greatly reduces the effluent management problem. The space environment permits a large pressure ratio for the MHD generator as an expansion engine and a reduction from the 20 atm pressure of the reactor to 1 atm exit was selected for the study. While a lower exit pressure could be adopted with consequent further improvement in enthalpy extraction, a performance mass trade-off study beyond the scope of Phase I would be needed. The system work indicates that the 1 atm adopted here is reasonable for the Phase I analysis. The effect of varying pressure has already been treated and reported (Ref. 9). With a pressure ratio of 20:1 and a magnetic field with a maximum value of 4T, the MHD generator analysis here is shown to produce specific energy extractions of at least 15MJ/kg while operating at the low, near constant sensible temperature of less than 1500K. This is to be contrasted with ratios of specific extractions of less than 2.5MJ/kg obtained with combustion driven linear MHD systems.

CHAPTER 2

SYSTEM DEFINITION

2.1 Overall System Requirements and Specifications

During the intensive period of space power system development in the 1960's, a major project (Ref. 1) to develop a hydrogen nuclear rocket system was set up and several engines were successfully ground tested. Known as the Nuclear Engine for Rocket Vehicle Application project from which the name NERVA is derived, extensive data were obtained and these have been used to specify a NERVA derivative reactor for use with a disk MHD generator. Additional information on which to base the specification was obtained from the space based, multi-megawatt MHD power system project conducted by Westinghouse for SDIO in which a disk MHD generator was also featured. (Refs. 2, 3)
Based on the use of hydrogen as the NERVA working fluid and materials of construction successfully employed in the test engines, Tables 1 through 3 have been prepared to (1) identify materials; and (2) provide mass and volume estimates for the major components. Table 1 deals with the heat source itself, the auxiliary shielding, the hydrogen cooling system, the heat rejection system and seed feed and management. In Table 2, the corresponding information is provided for the disk MHD generator and the associated electrical sub-systems. Finally, in Table 3, an estimate for the total dry mass of the complete power system, except for the hydrogen tank, is presented.

It should be pointed out that these Tables contain some degree of uncertainty, due primarily to the lack of mechanical, thermal and electrical MHD disk experimental data. Within the context of the study presented here, Tables 1 through 3 should be taken as a provisional system definition to provide a context for the generator and plasma analysis work. These Tables also provide a background for the definition and design of engineering experiments, the outcome of which will remove these uncertainties and so give an adequate engineering basis on which to determine system mass and develop a cost estimate.

In specifying the MHD generator and the auxiliary electrical subsystems, the power conditioning, magnet and energy storage sub-systems which it requires, Reference 2 was used to prepare Table 2. The selection of a disk generator configuration was made on the basis of conclusive experimental and analytical evidence from the Eindhoven Technical University (Ref. 7) and Tokyo Institute of Technology (Ref. 8) groups that this is preferred when non-equilibrium ionization has to be produced.

Table 1. Requirements and Specifications for NERVA Reactor and Associated Subsystems to Power 100MWe Open Cycle MHD Disk Generator

1. Heat Source	
Type	NERVA Derivative Reactor With Disk MHD
Materials	(See NERVA Reports)
Fuel	UC2-ZRC-C
Spectrum	Epithermal
Coolant	Hydrogen with Cesium Seed
Hydrogen Exit Temperature (K)	2975
Power Conversion	Open Cycle Nonequilibrium Disk MHD
Electrical Power (MW)	100
Heat Rejection Mode	Recuperative with Hydrogen Exhaust
Mass (kg)	2200
Volume (m^3)	1
2. Auxiliary Shielding	
Type	Beryllium, Zirconium
Configuration	Rings
Volume (m^3)	0.41
Mass (kg)	1200
3. Hydrogen Cooling System	
Type	Recuperative Cryogenic
Flow Rate (kg/s)	5.47
Inlet Pressure (atm)	63
Outlet Pressure (atm)	36
Inlet Temperature (K)	27
Outlet Temperature (K)	650
Mass and volume	Included in Component Data
4. Heat Rejection System	
Type	Hydrogen Effluent
Material	Carbon-Carbon Composite
Mass (kg)	35
5. Seed Feed and Management	
Type	Pumped Liquid Cesium
Cesium Seed (kg/s)	0.013
Material	Aluminum
Mass (less Seed)	Function of Run Time

Table 2. Requirements and Specifications for MHD Generator and Associated Electrical Sub-Systems.

1. MHD Disk Generator.	
Type	Open Cycle Non-equilibrium Disk MHD
Working Fluid	Cesium Seeded Hydrogen Plasma
Power (MWe)	100
Voltage (kV DC)	40
Materials	Aluminum Oxide Brick and Felt, Tungsten, Boron Nitride, Composites, Aluminum, Super Alloy, Titanium
Mass (kg)	2000
Volume (m^3)	1.6
2. Power Conditioning	
Type	DC-DC Boost Converter
Number of P.C. Units	12
Device Technology	GTOs
Voltage Output (kV)	100
Heat Dissipation (kW)	2200
Efficiency (%)	97.8
Mass (kg)	1900
3. Magnet	
Type	Cryogenic Split Pair Coils/Aluminum Conductor, Liquid Hydrogen Cooled
Dimensions	
Radius (m)	0.8
Gap (m)	0.2
Material	High Purity, Aluminum, Super Alloy, Insulation
Field Strength (T)	4 Peak, 3.5 Average
Power Consumption (kW)	70
Mass (kg)	1500
4. Energy Storage	
Type	Battery/Magnet Power System
Mass (Entire Storage) (kg)	90

It is not sufficient, however, just to have a compatible heat source and good mixing of the cesium seed material to achieve high performance generator operation. There are two additional considerations which have to be taken into account if the expected high performance is to be obtained. The first is to ensure that the seed is fully ionized and, as has been shown by Shioda and his colleagues at the Tokyo Institute of Technology, this leads to the adoption of much lower seed concentrations than were considered during most of the development of non-equilibrium generators, a typical value being around 10^{-5} molar fraction of cesium. This issue is discussed in detail in Chapter 3; to

provide some indication of the effect of non-uniformities, a plasma non-uniformity parameter established by Louis and Klepeis (Ref. 25) was used in the system studies. This parameter, designated a, as formally established in Chapter 3, is a measure of the degree to which the ionization of cesium seed falls short of 100%.

The second critical consideration is the method of loading the MHD generator. In prior studies, investigators have had difficulty in obtaining high performance when a single load was used. As the disk generator is a radial Hall configuration, it may be supposed that the two-terminal characteristic of the Hall machine can be advantageously utilized to avoid the electrical complexities of multiple terminals associated with linear machines. However, this leads to difficulties in developing the needed non-equilibrium conditions in the plasma, regardless of working fluid.

A major contribution to non-equilibrium MHD generation operation by the investigators involved in the Phase I study has been to point out that multiple loading is a basic requirement (Ref. 9). This may be explained qualitatively by observing that the MHD generator has to be loaded so that the entry portion can Joule heat the electrons to the required temperature and this typically utilizes about 15% of the active generator length (radius). The inclusion of a second anode enables the loading on the inter-anode portion to be adjusted for the required ionization conditions and the remainder of the channel to be loaded for optimum power extraction. In this study, two loads, one between the first anode and cathode and the other between the second anode and cathode were utilized throughout the study. Analytical support for this result appears in Chapter 4.

The requirement for power conditioning to match the generator output to the system busbar (taken here to be 100kV DC) implies, at the power level involved, that a modular power electronics approach be used. From the electrical conversion point of view, there is thus no intrinsic merit in providing a two-terminal input to the power conditioning system and the improvement in generator performance, as verified later in this Chapter, fully justifies the allocation of the power conditioning modules to two separate loads.

For space power systems in which DC is generated and, amongst which MHD is, of course, included, the mass of the power conditioning to provide the desired DC busbar voltage penalizes the overall system mass relative to that obtained with rectifiers and regulators in the case of rotating AC machine systems. The high voltage capability of the MHD disk generator has already been shown analytically (Ref. 9) and confirmed in both equilibrium and non-equilibrium experimental devices. The maximum wall voltage stress which can be supported by the cesium seeded hydrogen plasma required in the disk MHD generator has, however, yet to be established and is a specific topic for future investigation. Based on available breakdown data and considerations discussed in later Chapters, a limit of 125 KV/m was tentatively established and used in the system studies. As with other types of MHD generator, the supportable Hall voltage is clearly a limiting parameter which will feature importantly in generator design.

Regardless of the limiting voltage stress, the high voltage capability of the MHD disk generator introduces important new possibilities for reducing the mass of the power conditioning system. Specifically, DC-AC-DC schemes involving what may be termed classic inverters and a step-up transformer may be replaced by chopper type direct DC-DC converters widely used in low voltage versions in electric traction and other applications when the source to busbar voltage ratio is not more than about 1:3 (or 3:1). Provided that disk generator can produce output voltages in the range 30-50kV, significantly lower mass power conditioning than was hitherto considered possible can be developed to cover the busbar voltage range 10-100kV. The significant part is that the most massive component, the step-up transformer, can be eliminated and the only remaining major passive component is the interfacing inductor between the generator and the converter input. Further discussion of the use of chopper circuits in the power conditioning sub-system in given in Section 2.4 and results presented in this Section were used to estimate the power conditioning mass in Tables 2 and 3.

The remaining major electrical sub-system is the magnet and this, following the earlier Westinghouse design (Ref. 2) prepared by the MIT National Magnet Laboratory, consists of two ultra-high purity aluminum coils operated in the hyperconducting mode. The magnet is battery powered throughout the entire pulse period to avoid the complexity of switching the magnet and load to achieve generator self-excitation. The battery is, in any event, needed to ensure that full magnetic field is available to initially ionize the plasma. The estimated mass of around 90kg for energy storage of about 6kW hr is a minor contributor to the overall system mass. For a fuller treatment of all major components, Reference 2 should be consulted.

2.2 Requirements and Specifications for the MHD Generator

As has long been recognized, starting with the pioneering work of Kerrebrock (Ref. 21), the attraction of non-equilibrium ionization is that it separates the thermodynamic performance of the MHD generator as a heat engine from the development of the required electrical conductivity. The NERVA reactor is, in contrast to combustion systems, an excellent heat source for the light, high γ hydrogen working fluid desirable on thermodynamic grounds yet avoids the introduction of contaminants which will adversely affect the electrical conductivity. These factors are the basis for the impressive generator performance results presented in this Chapter.

The space based, multi-megawatt MHD power system Phase I studies conducted by STD Research Corporation (Ref. 4), TRW (Ref. 5), Westinghouse Corporation (Refs. 2, 3) and Textron (Ref. 6) for SDIO, used a common specification in that the required output was 100MW of electrical power at a DC busbar voltage of 100kV, with pulse operation up to a maximum total run time of 1000s. This requirement has also been applied to other systems, such as the hyperconducting alternator, also being worked on by Westinghouse Corporation. Accordingly, to facilitate comparison, the same output ratings were selected

for this project, with the proviso that, to the extent possible within the resources available, the consequences of changing the power level, busbar voltage and run time could be explored.

An estimate of the overall system mass for the Reference Case defined in this Chapter, was made and is presented in Table 3. The dry mass of the system, excluding the hydrogen tank, was found to be approximately 0.1 kg/kW. For operating times typical of the systems considered here. With a hydrogen flow of 5.7 kg/sec., this yields an overall specific mass of 13.5 MJ/kg, an estimate which can only be refined when Phase II results are available but which indicates the potential of this system to provide exceedingly low specific mass in the multi-megawatt range.

Table 3. System Mass Estimate

Component	Metric Tons
Power Source	2.2
MHD Generator	2.1
Magnet	1.5
Energy Storage	0.1
Heat Rejection	0.04
Aux. Shielding	1.2
Hydrogen Pump	0.4
Power Conditioning	2.1
Misc. Structure	0.43
Controls	0.08
Total Dry Mass (less Hydrogen Tank)	9.95

2.3 Thermodynamic Analysis

The approach followed in implementing the system effort was first to establish the parameter values for high performance operation and then to seek confirmation that these were compatible with a stable plasma which implies that the plasma is essentially fully ionized. Motivation for this approach, as already indicated, came from the pioneering work of the late Professor Louis (Refs. 24, 25) and the results obtained by the leading research groups dealing with non-equilibrium MHD generators. These are headed respectively by Professor L. Th. Rietjens and Professor S. Shioda at the Eindhoven Technical University in the Netherlands and the Tokyo Institute of Technology in Japan. The work by these groups to date has the important limitation relative to this project that it has dealt only with potassium and cesium seeded noble gases (argon and helium). Some consideration has been given to non-equilibrium ionization in hydrogen, particularly by Rosa (Ref. 10), and his discussion of the realization of stable non-equilibrium ionization ends with the statement that:

"However, it is not yet clear that useful results cannot be obtained by employing a high Mach number together with a low $\Omega\tau$, a low seed concentration, and/or by favoring geometries, such as the disk, which avoid segmented electrodes". . .

but he provides no analytical support for these conclusions. Faced with this situation, it appeared best in Phase I to pursue the general directions indicated by Rosa and this, of course, was supported by experience gained in prior studies of the concept.

The requirements and specifications presented in Tables 1 and 2 and the NERVA disk MHD system shown in block diagram form in Figure 2, were used to generate a set of parameters which could reasonably be expected to lead to the level of performance

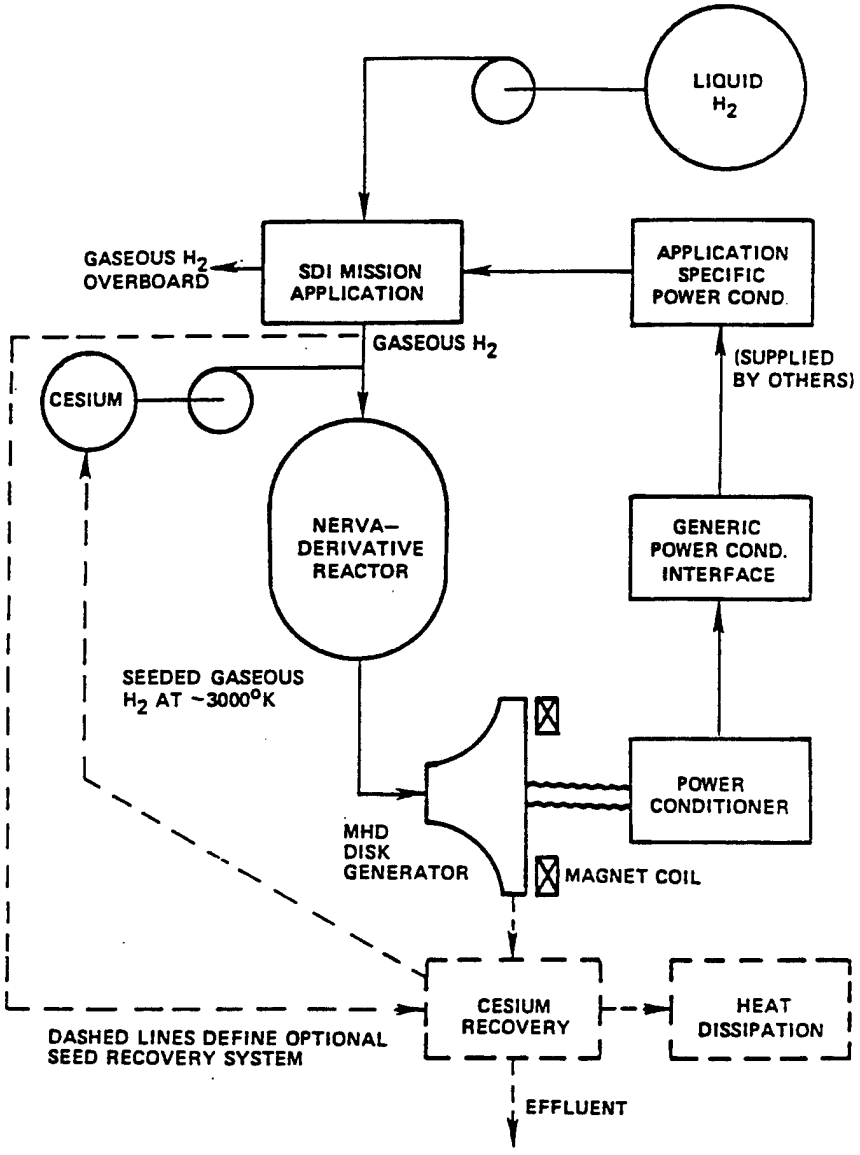

Fig. 2. Major Components, Flows and Interfaces for MHD Disk NERVA Reactor System.

desired on the basis of 100% seed ionization (designated the "Full Ionization Case"). The disk generator power output was set at 107MW so that, with a 93.5% assumed efficiency for the power conditioning sub-system, an overall busbar power of 100MW would be obtained. The generator was assumed to have two anodes as described in the preceding section, with a magnetic field of 4T in the inter-anode region and 3.5T for the rest of the machine. These numbers were selected from prior work as was the seed faction of 1.5×10^{-5} molar fraction which was also consistent with the helium results of Shioda and his colleagues. The reactor stagnation pressure of 20 atm was also selected based both on reactor and prior disk generator analysis experience.

In view of the large number of parameters involved, two categories of parameters were established, the first being those which were fixed throughout the analysis with values chosen on the basis of prior experience, and second being those which were varied to enable a high performance, Full Ionization Case to be identified. Table 4 lists these parameters amongst which stagnation pressure, magnetic field, working fluid, seed fraction, wall temperature and total generator DC output power were fixed. The exploration in parameter space for the best obtainable performance was primarily conducted by varying the inlet Mach number and the two loading factors until an enthalpy extraction significantly in excess of 40% was obtained.

These one-dimensional system calculations were conducted using the Westinghouse proprietary Systems Performance Analysis (SPA) code assembled as shown in Figure 3 which also identifies all input and output quantities. While this procedure is not a full system optimization, the values obtained are considered to be typical of those to be found in a high performance system. The values obtained, however, are based on power system analysis experience (Ref. 2, 9) and it is unlikely that they would be changed significantly if a full optimization procedure were to be conducted using the same model. The additional effort required to refine this process was not considered to be justifiable in Phase I, during most of which the plasma stability regime for hydrogen depicted in Figure 20 was not available and in lieu of which the corresponding Shioda result for helium and also given in Figure 20 had to be used as a guide.

The next step was to explore the effect of less than complete cesium ionization and this was done by introducing the plasma non-uniformity parameter of Louis and Klepeis as already discussed and further treated in Section 3.4, dealing with the effects of non-uniformities and fluctuations. Figure 4 shows the effect of varying this non-uniformity parameter while holding the total generator output at 100MW using the same fixed conditions as for the full ionization case. As was to be expected, the enthalpy extraction falls off and the radius of the machine increases. From these results a "Reference Case" with $a = 0.01$ was selected and the remaining Table 4 parameters calculated as shown. Using this value of a corresponds to 91% ionization, about the Figure 4 lower limit which can be tolerated before performance begins to be significantly adversely affected.

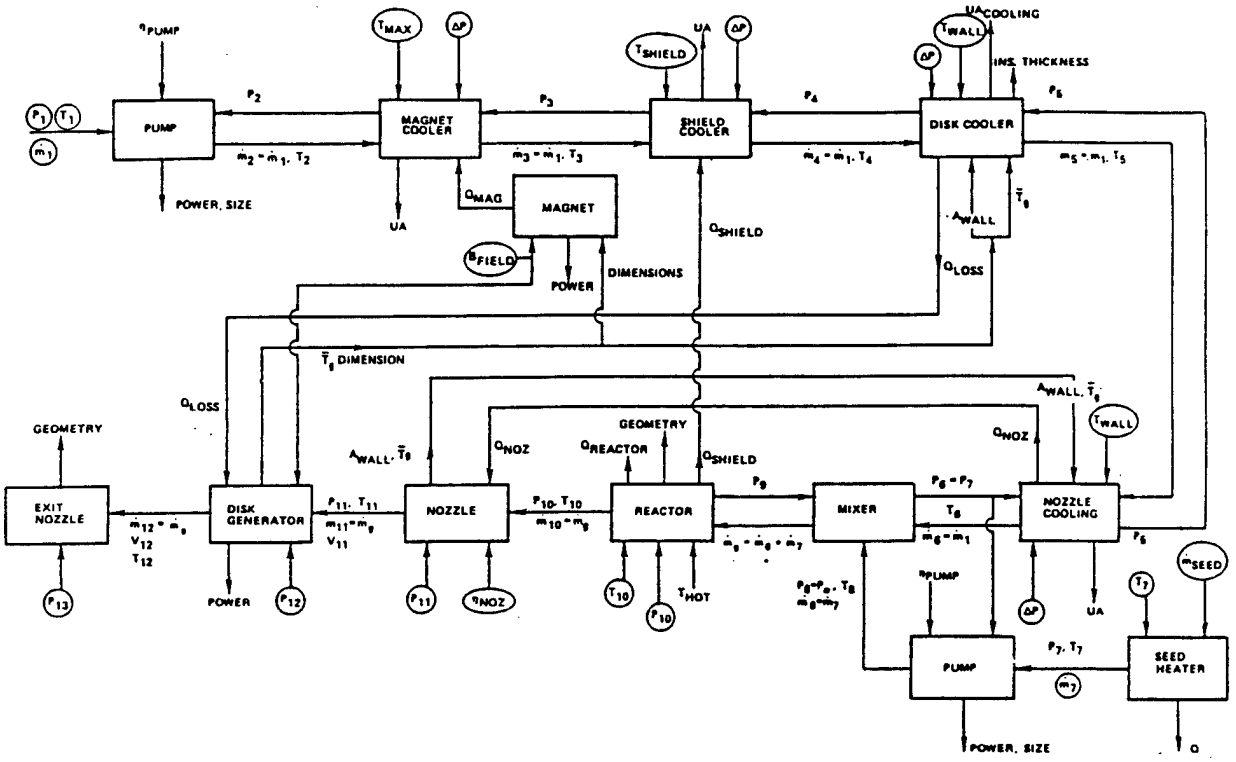

Fig. 3. Computer Simulation of NERVA Reactor MHD Disk System.

Table 4. Design Conditions for MHD Disk Generator

	Full Ionization Case	Reference Case
Stagnation Pressure (atm)	20	20
Inlet Mach Number	3.2	3.2
Magnetic Field at the Anode (T)	4.0	4.0
Magnetic Field at the Cathode (T)	3.5	3.5
Working Fluid	H_2 + Cs	H_2 + Cs
Seed Fraction	1.5×10^{-5}	1.5×10^{-5}
Plasma Non-Uniformity Parameter	0	0.01
Loading Factor between Anodes	0.55	0.55
Loading Factor immediately after Second Anode	0.72	0.725
Wall Temperature (K)	2000	2000
Total Generator DC Output Power (MW)	107	107

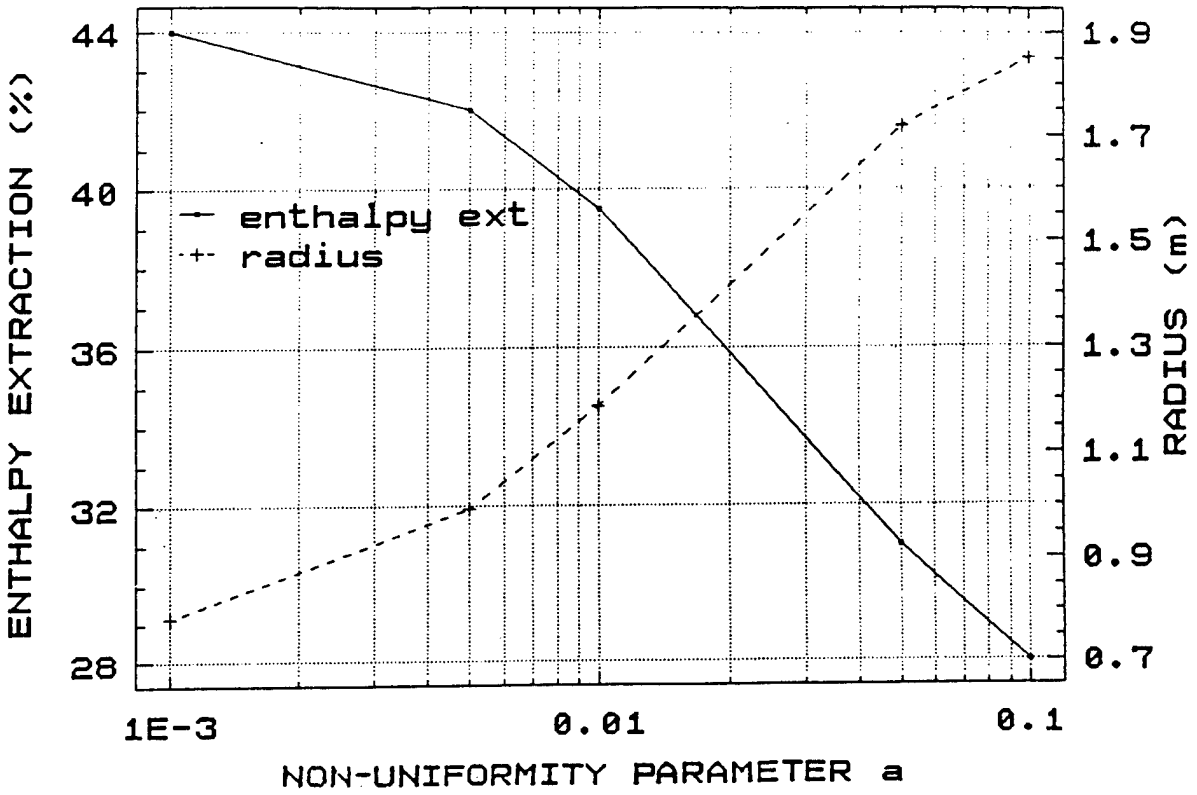

Fig. 4. Enthalpy Extraction and Outer Radius Disk as a Function of Plasma Non-Uniformity Parameter.

The operating conditions for the two disk cases as a function of radius were calculated using the SPA code and the results are summarized for convenience in Table 5 and shown fully in Figures 5 - 14. Referring to Table 5, the enthalpy extraction for the Full Ionization and Reference Cases were 44% and 39% respectively, requiring corresponding thermal inputs of 245MW and 270MW. Currents, radial electrical field, maximum Hall voltage, inter-anode voltage are presented in Table 5 to indicate the electrical performance. The plasma behavior is represented by the Hall co-efficient, β the effective conductivity and the electron temperature. The Table is completed with the fluid mechanics parameters, outlet Mach number, mass flow, pressure loss, heat loss and key dimensions.

The spatial behavior of the Hall Parameter β electron temperature, electrical efficiency, power, voltage, static pressure, Mach number and swirl as a function of radius are depicted in Figures 5 through 9 for the full ionization case and Figures 10-14 for the reference case. On each of these Figures, the local loading also appears to provide a parameter comparison and also to show how these quantities behave through the electrical discontinuity created by the change of loading. Particular aspects of the behavior which should be pointed out are:

1. Power and voltage are nearly linear functions of radius.
2. The electron temperature reaches the level at which hydrogen can be ionized but this can be accommodated with some loading adjustments which will not affect the overall performance.
3. The Hall parameter at the exit is 18 in the Full Ionization Case and 14.6 in the Reference Case. These may at first appear to be large values but it may be pointed out that Shioda has already measured an effective Hall parameter of ≈ 14 in the course of his studies of cesium seeded helium disk generators. This Shioda result, in fact, greatly influenced the choice of the parameter a = 0.01 for the Reference Case.
4. As is to be expected, the radial dimension of the cathode for the Reference Case is increased by about 15% over the Full Ionization Case but the result is still an exceedingly compact generator.

Table 5. Summary of MHD Disk Generator Performance and Operating Conditions

	Full Ionization Case	Reference Case
Thermal Input (MW)	245	270
Enthalpy Extraction (%)	44	39
Isentropic Efficiency (%)	60	59
Current at First Anode (A)	2036	2035
Current at Cathode (A)	2779	2778
Maximum Er (Inter Anode Region) (kV/M)	120	90
Hall Voltage First Anode to Cathode (kV)	40.6	40.3
Inter-Anode Voltage (kV)	7.78	6.75
Power Density (Average) (MW/m3)	526	500
Electron Temperature Range (K)	8200-5000	8200-5000
Maximum Effective Beta	18.8	14.6
Maximum Effective Conductivity (S/m)	7.89	6.43
Mass Flow (kg/s)	5.47	5.47
Outlet Mach Number	1.15	1.15
Pressure Loss (atm)	0.02	0.02
Heat Loss (MW)	0.4	0.7
Radius of First Anode (m)	0.18	0.18
Radius of Second Anode (m)	0.255	0.265
Radius of Cathode (m)	0.695	0.78
Channel Height at First Anode (m)	0.070	0.070
Channel Height at Cathode (m)	0.174	0.159

The Reference Case specified in Tables 4 and 5 and analyzed on a one-dimensional basis by using the SPA code, illustrates the impressive performance attainable with the cesium seeded, hydrogen non-equilibrium disk MHD generator. Except under conditions where the DC output level and power quality are acceptable for direct application to a load, however, power conditioning is required to complete what can truly be described as an "electromagnetic turbine-generator".

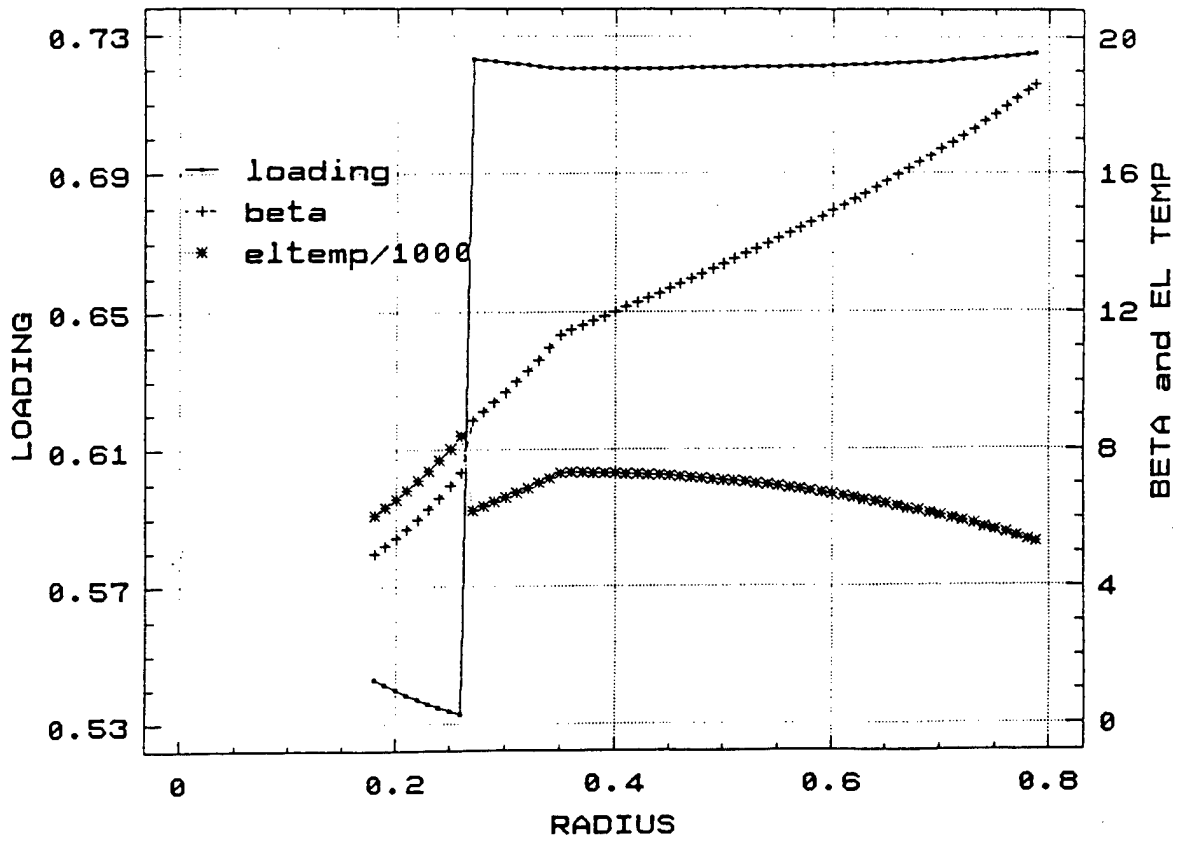

Fig. 5. Loading, Beta, and Electron Temperature as a Function of Radius for Full Ionization Case.

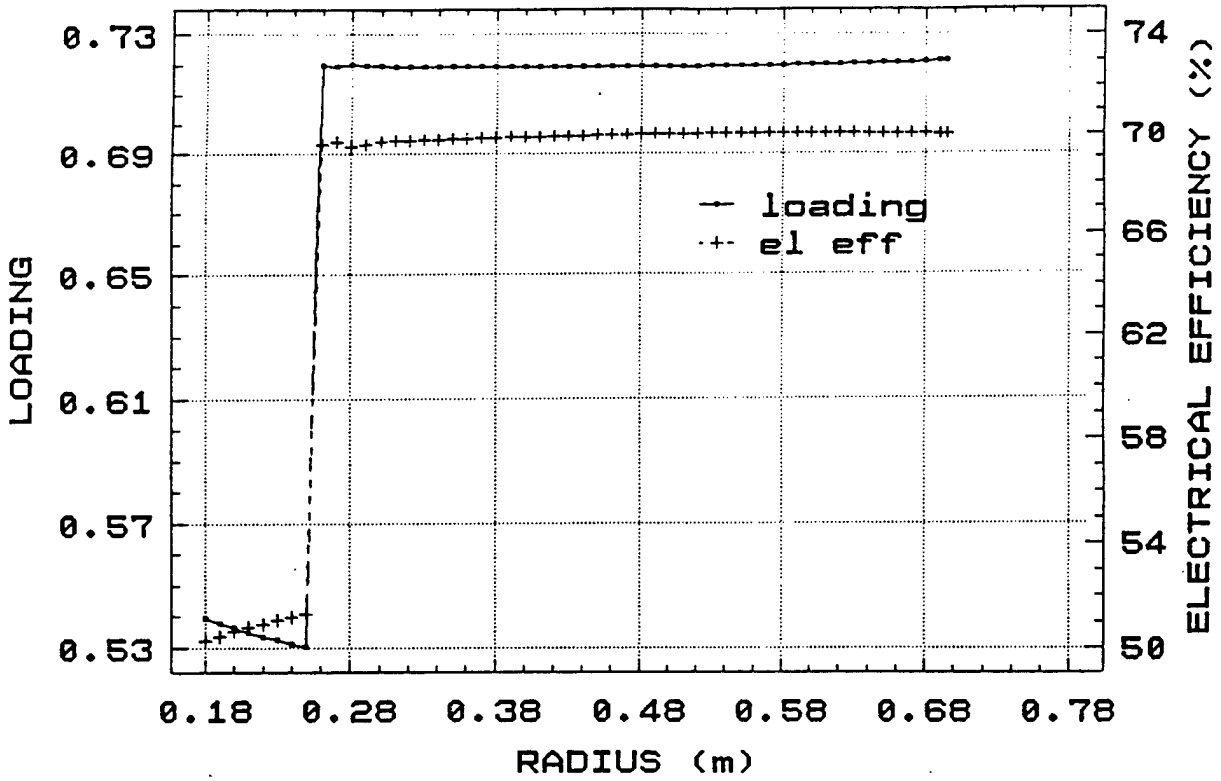

Fig. 6. Loading and Electrical Efficiency As a Function of Radius for Full Ionization Case.

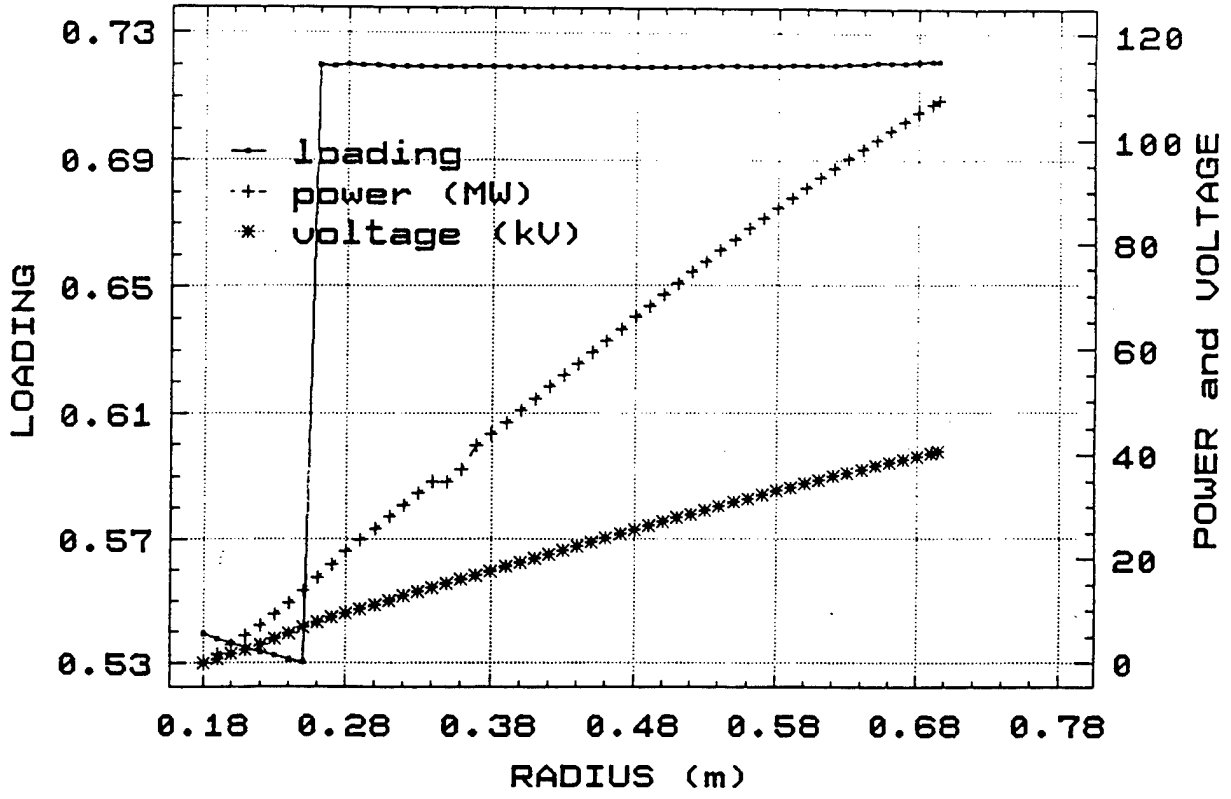

Fig. 7. Loading, Power and Voltage as a Function of Radius for Full Ionization Case.

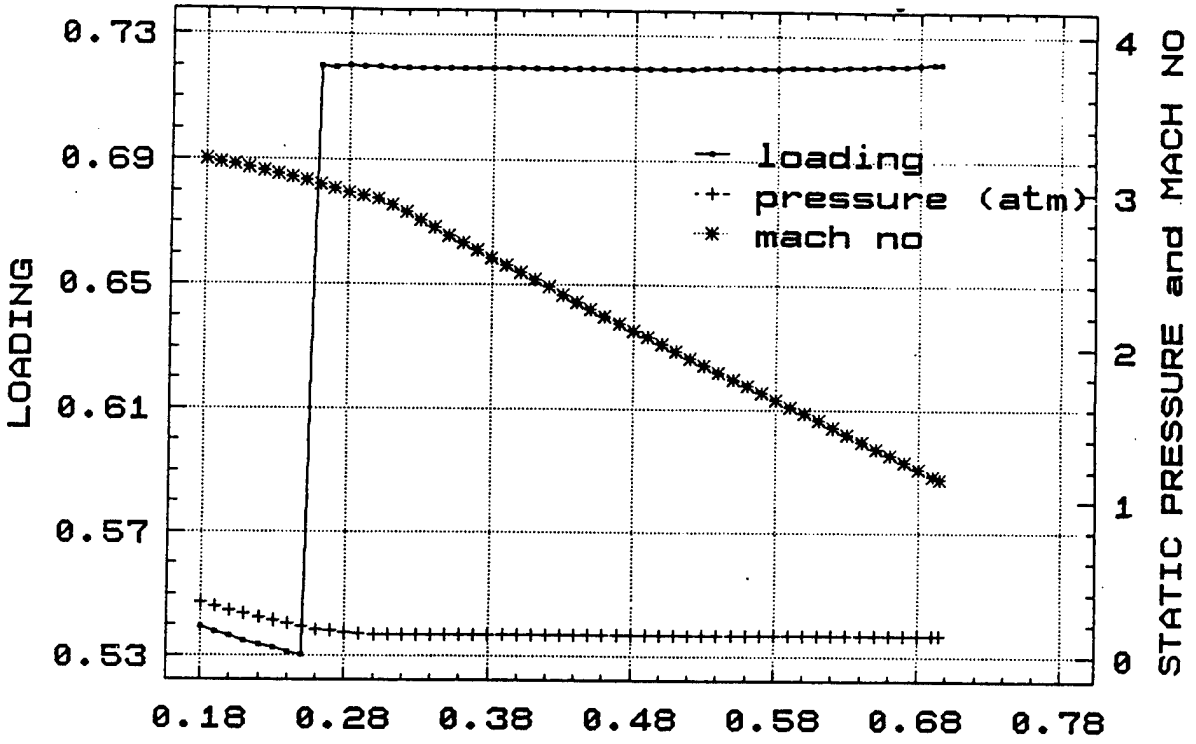

Fig. 8. Loading, Static Pressure and Mach Number as a Function of Radius for Full Ionization Case.

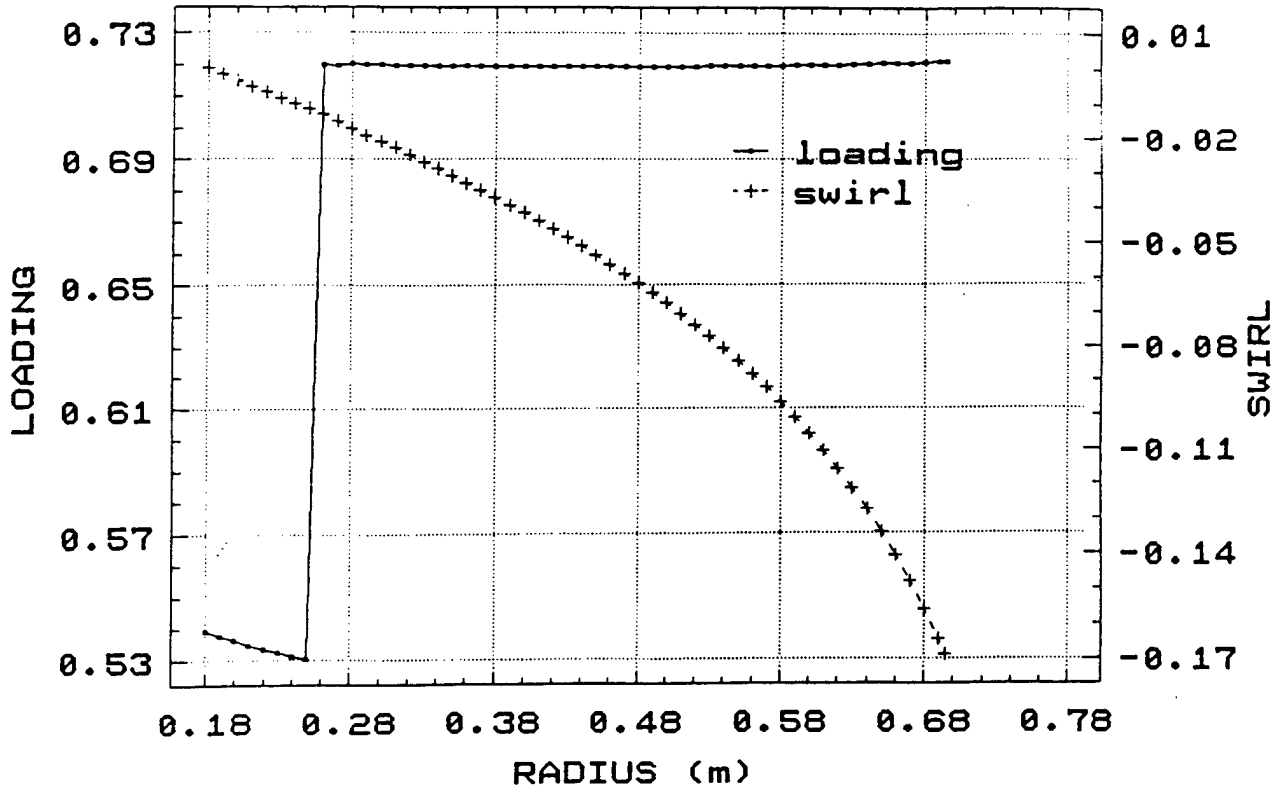

Fig. 9. Loading and Swirl as a Function of Radius for Full Ionization Case.

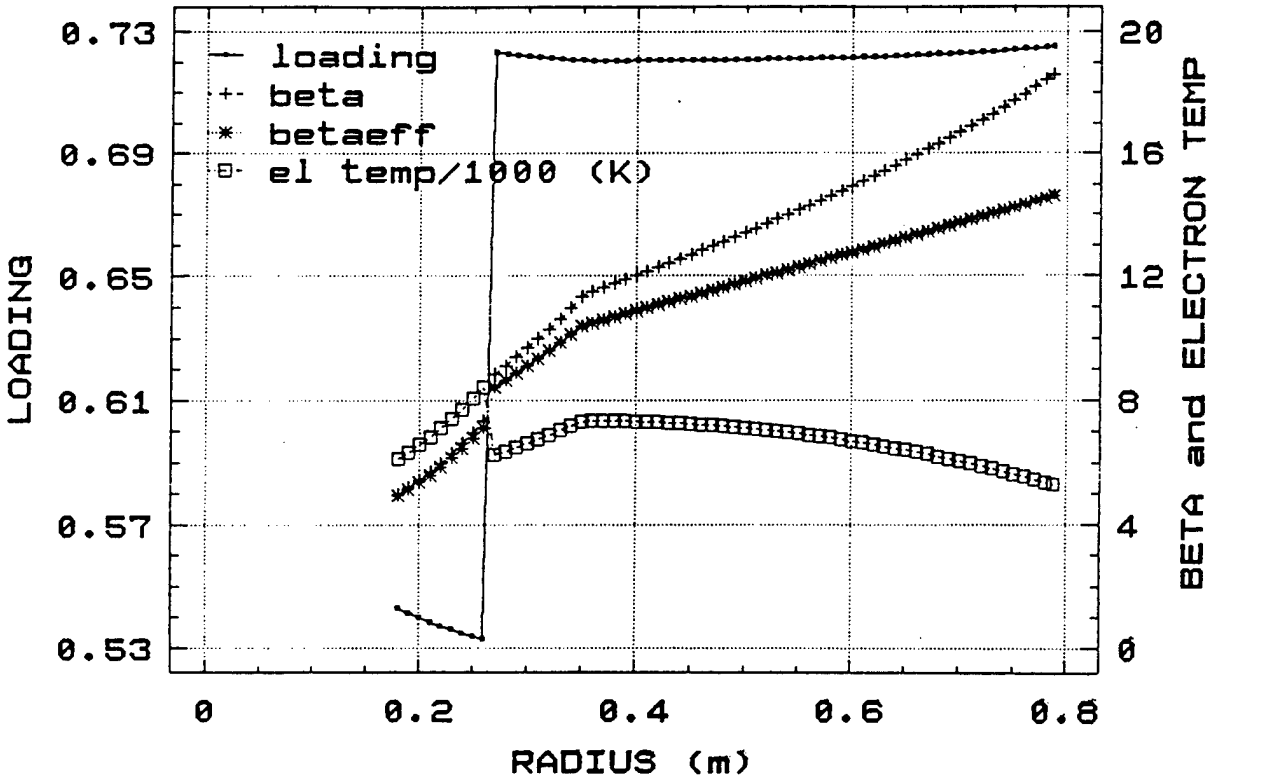

Fig. 10. Loading, Beta, Beta-Effective and Electron Temperature as a Function of Radius for Reference Case.

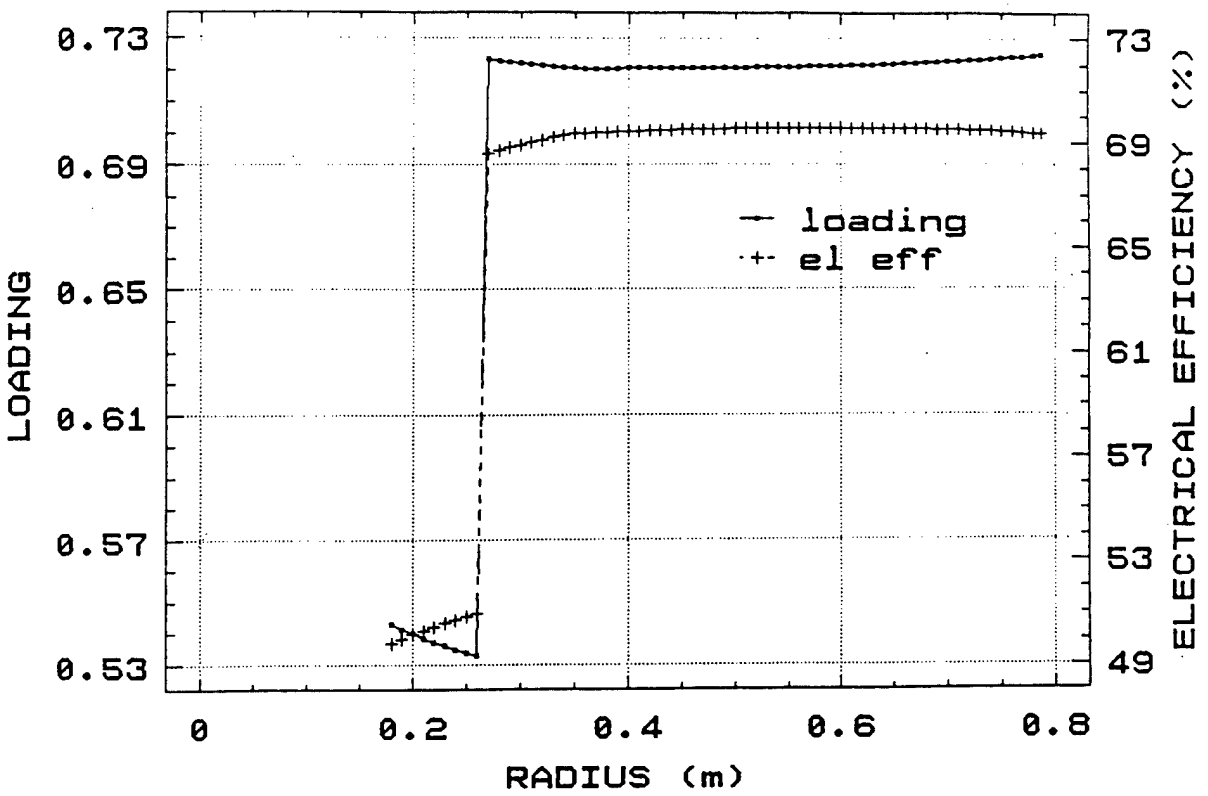

Fig. 11. Loading and Electrical Efficiency As a Function of Radius for Reference Case.

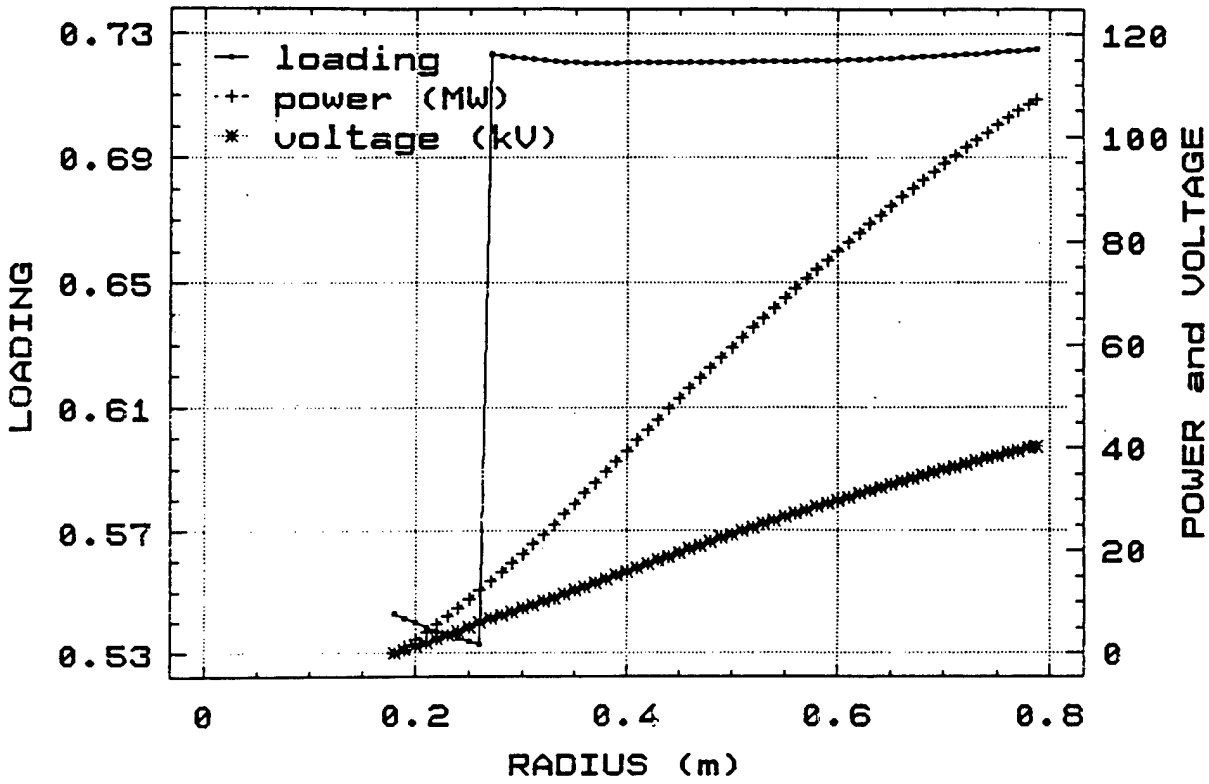

Fig. 12. Loading, Power and Voltage as a Function of Radius for Reference Case.

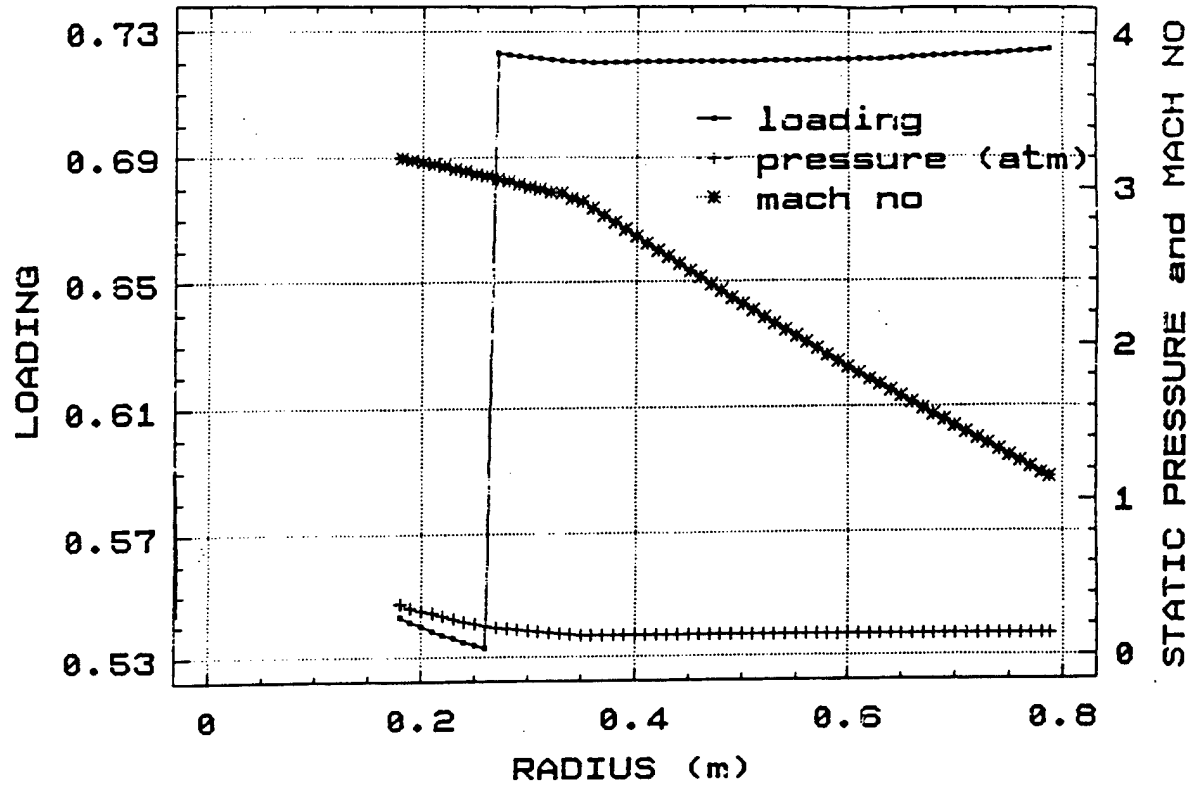

Fig. 13. Loading, Static Pressure and Mach Number as a Function of Radius for Reference Case.

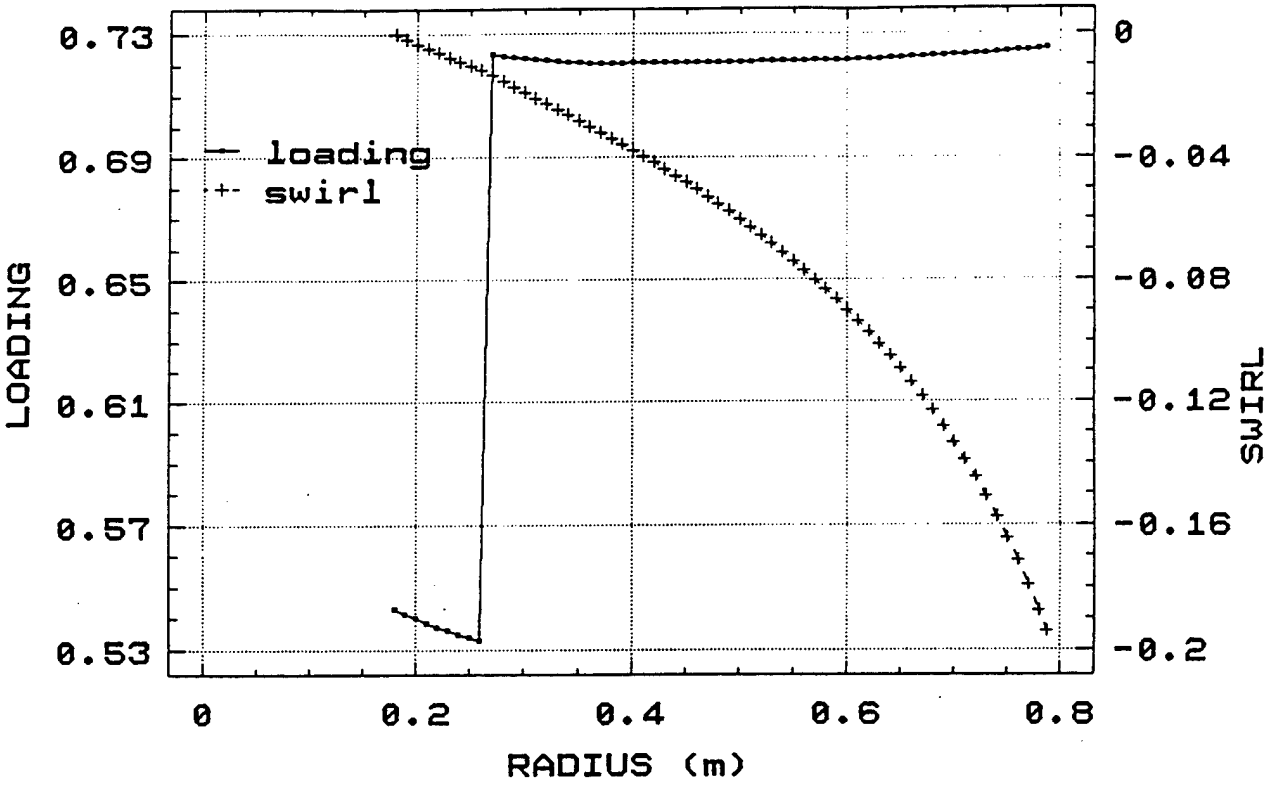

Fig. 14. Loading and Swirl as a Function of Radius for Reference Case.

The establishment of a competitive position for the NERVA disk MHD disk generator system considered here depends in large measure on the development of a power conditioning system which is not the dominating contributor to the overall system mass as was found in the SDIO studies cited earlier. Accordingly, to complete this Section devoted to system analysis, the power conditioning issue is now treated to show how the characteristics of the Reference Case can be exploited to provide a major improvement in power conditioning.

2.4 Power Conditioning

Prior SDIO MHD system studies (Refs. 3, 4, 5, 6) all involved a voltage ratio which was much too high for true DC-DC converters, often referred to as "choppers", to be used. The approach had to be based on DC-AC conversion, followed by AC transformation and re-rectification to DC. Not only did this introduce a transformer, a relatively massive component, but also required parallel, and in some cases also series connection, of devices or converters in the DC-AC stage. This latter requirement arises from the limited current and voltage ratings of individual devices. Further, the well-established advantage of bridge connection for AC-DC-AC topologies approximately doubled the device count.

The Reference Case utilized two anodes and accordingly requires two separate power conditioning sections as shown in Figure 15. The DC input to converter #1 is the full 40.3kV and its full load current is 2.035KA. The second converter is connected between the second anode and the cathode and the corresponding values are 33.5kV and 743A respectively. Assuming delivery into a 100kV busbar, this corresponds to voltage ratios of 2.48 and 2.98 for the two units, giving values of 1.67 and 1.50 respectively for the DC-DC converter average value term 1/A.

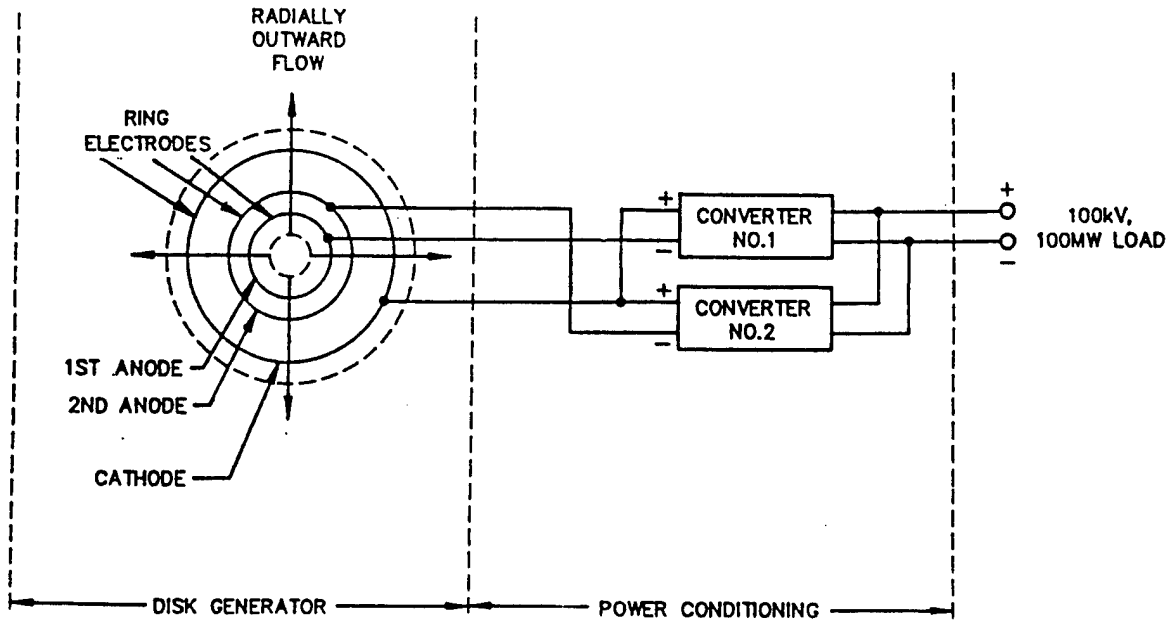

Fig. 15. Power Conditioning System Configuration

With the advent of the gate controlled thyristor or GTO, low voltage DC-DC converters, usually of the buck or voltage reducing type, have been widely employed in motor control, particularly in traction applications where DC motors are still widely used. The boost converter, shown in basic circuit terms in Figure 16a and with its actual circuit elements in Figure 16b, is also possible when voltage step-up is required. As a current sourced converter, it has found application where DC busbar voltages have to be regulated to a specified level from a variable, somewhat lower voltage source. In the development of true DC-DC converters, little attention has been paid to high voltage versions in which the controlled switches and the blocking diodes have to be series connected to meet the voltage requirement. Extensive experience does exist, however, both with series-connection thyristor and diode operation in high voltage (HVDC) transmission systems and no difficulty is foreseen in applying this to the specific conditions of the space environment. Further, experience is now being gained with the series operation of GTOs, both for HVDC and other large scale converter systems, such as those required in superconducting magnetic energy storage.

The A values applicable to the Reference Case indicate from experience with true DC-DC converters that the topology of choice is indeed a boost-type converter. This could be implemented using field effect (MOSFET) transistors, bi-polar transistors, or GTOs as switching devices. As self or forced commutation of the switches is required, thyristors are not appropriate candidates in this case. Power ratings of transistors for switching applications are so low, that the number of devices needed to process 100MW would be enormous and serious questions of reliability would arise. On the other hand, GTOs are available at high power ratings, typically 4500V/2500A (switching) and these are realized on a 75mm silicon slice. With larger GTOs becoming available, the preliminary design of the converter undertaken here is based on a 100mm, 6kV/4kA GTO. This choice also facilitates comparison with the study reported in Reference 2 where a similar conversion requirement from a low voltage disk generator was addressed using the classic DC-AC-DC inverter approach.

Applying the usual peak voltage, peak current and rms current criteria to boost converters, it is evident that a single series GTO string can be employed. For both converter #1, 18 series GTO's are required, as are 18 series diodes as shown in Figure 16c. In this preliminary calculation, the same GTOs and diodes have been assumed for both converter units but some advantage may be gained by using a reduced current rating in unit 2 which is only required to handle about 750A.

The main components to be considered from performance and mass viewpoints in the preliminary design in addition to the switches, are the snubbers, the input series inductance to control input current ripple and the output capacitor to limit output voltage ripple. As DC-DC converters with the common positive input polarity, only parallel connection of the output side is possible and Figure 16c reflects this common positive line requirement. While in this preliminary design, the arrangements internally for

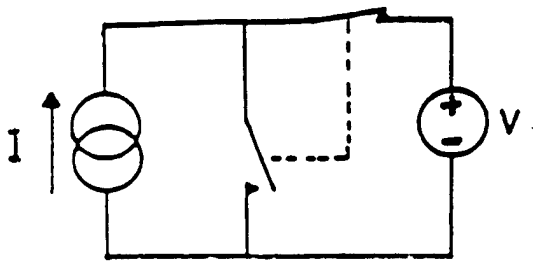

a. Idealized Circuit

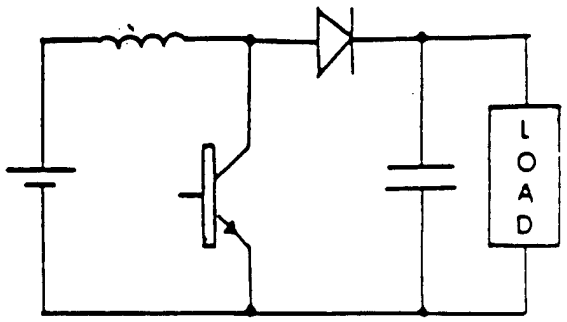

b. Basic Elements

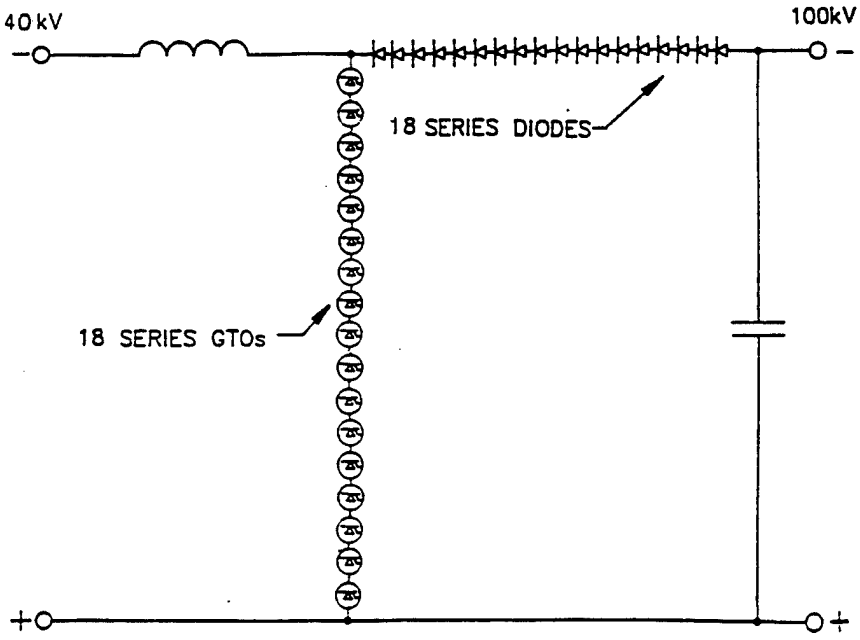

c. Circuit for Converter Module (without snubber and controls)

Fig. 16. Boost Type DC-DC Converter

converters #1 and 2 are identical, advantage has been taken of the reduced current in converter #2 in the design of the current sourcing interface inductor.

A final design consideration is the operating frequency which in DC-DC converters, as DC-AC-DC inverters, is the principal operating variable influencing mass. Frequency influences the inductor and filter mass and also the coolant mass needed for active devices and their snubber networks. Inductor and filter mass decrease with increasing frequency while coolant mass increases (Ref. 12). For the conditions considered here, GTOs set the upper frequency bound because of heat transfer limitation resulting from their packaging and limited operating temperature range, as well as their acceptable switching efficiency. The maximum allowance dissipation of 6kW/device allowed for the GTOs assumed in this study limited the operating frequency to 400Hz.

At 400Hz, the current sourcing inductors can readily absorb their own heat losses and this was assumed in the design although, in future, it would be appropriate to consider fabricating these from ultra-high purity aluminum as proposed for use in the magnet coils and cryogenically cool them to greatly reduce dissipation. Using copper and aluminum current densities of 7500 and 5500A/in^2 respectively, aluminum was found to give the lighter inductance masses. A temperature swing of -40 C to 300 C was used so as not to compromise the operation of the semi-conductor devices over the maximum operating time of the system.

Using mass and loss estimating procedures already established in prior work (Refs. 2, 12), estimates were prepared for the Figure 16 system. The mass and efficiency were estimated to be 1900/kg and 97.8% respectively. The mass number is about four times improvement over the Reference 2 calculation, a result which is reasonable as the transformer, 50% of the mass of that design, and more than half of the GTO's and 80% of the diodes have been eliminated. The efficiency value is typical of DC-DC convertors and significantly better than was assumed in the SPA calculations for which it was not available.

A more detailed design than was possible with Phase I resources and the availability of Phase II results should lead to further improvement in the power conditioning for both mass and efficiency values. For the present, it may be included that the high voltage disk, for a wide range of DC busbar voltages, offers very substantial mass reduction for the associated power conditioning subsystem.

CHAPTER 3

PLASMA MODELING

As explained in Chapters 1 and 2, the analysis of the hydrogen-driven disk generator started with simple models for the basic operating parameters.

The Hydrogen-driven disk was first analyzed as an ideal expansion engine to define loading and efficiency requirements for a high-performance design. Then a one-dimensional computation of the disk generator electrical and gasdynamic performance with friction and heat transfer was carried out to arrive at an attractive design from the system point of view. Plasma properties for this computation were obtained by a two-temperature model with published data for electron energy loss factors and collision cross sections for momentum transfer. The low seed fraction and high electron temperature lead to 100% ionization of the seed, and this case is presented in Chapter 2 as the "Full Ionization Case". The effects of potentially important nonideal processes (more than were contemplated at the outset of the work) on generator performance were then estimated within the operating regime. Finally, the simple models were re-executed with the most important nonideal processes to give a final design of the full scale generator, which is presented in Chapter 2 as the "Reference Case".

Many interdependent physical mechanisms act simultaneously on the flowing plasma to affect the local behavior and the overall characteristics of nonequilibrium $\vec{J} \times \vec{B}$ devices. By local behavior we mean the spatial distribution and the time dependence of the current density $\vec{J}$, the electric field $\vec{E}$, the electron Temperature T_e, the electron concentration n_e, and the Ohmic heating $\vec{J} \cdot (\vec{E} + \vec{U} \times \vec{B})$. By overall characteristics we mean the internal resistance, efficiency, and operating voltage of the device. Very important among these mechanisms are:

(1) The anisotropic property of the plasma as a conducting medium in the presence of a magnetic field. The effect of this mechanism is usually defined by the effective value of the Hall parameter β_{eff}.

(2) The nonlinearity of the plasma as a conducting medium due to electron heating. The magnitude of this effect depends on the energy loss factor δ_{eff} of the operating fluid and the loading conditions; more specifically, the local elevation of the electron temperature depends upon the local Ohmic dissipation and upon the local rates of electron energy convection, and of energy transport between the electrons and the heavy particles due to elastic and inelastic collisions.

(3) The instability of the plasma as a conducting medium that can result in local fluctuations of its transport properties, and therefore time-dependent current and potential distribution in the device.

(4) Finite reaction rates for the processes of ionization, dissociation, and recombination and their effect on the spatial variation of plasma properties (*i.e.,* the nonuniformities) in nonequilibrium devices.
(5) The gas temperature and gas velocity variations in the boundary layers that are developed on the the sidewalls.
(6) Electrode surface and sheath characteristics and their effect upon the local behavior in the electrode boundary regions.
(7) Thermal and concentration diffusion due to the electron temperature and pressure gradients ∇T_e and ∇p_e that can be sustained in nonequilibrium $\vec{J} \times \vec{B}$ devices.

In this study we have examined the above mechanisms (1) – (5), as well as effects of magnetic Reynolds number, ion slip, insulator wall breakdown, and radiation losses using existing computer codes developed at STD Research Corporation. We have also surveyed the literature on hydrogen plasma properties and have incorporated these data in the analyses where appropriate. The significant findings from the present modeling effort were the following:

(A) The use in the system calculations of the two-temperature model for electron nonequilibrium based on published data for the electron energy loss factor in 300 K hydrogen is adequate to find feasible operating conditions for the disk generator at the electron temperatures considered. While it is still important to quantify differences in the electron energy loss factor in hot gases (which should be accomplished in future experiments described in Chapter 4) such differences are unlikely to be overriding because, unlike other diatomic molecules such as N_2 and CO, The cross sections for exciting inelastic processes is very small at the electron temperatures of interest. In particular, the onset of vibrational excitation by electron impact occurs in H_2 above the 0.53 eV energy of the first vibrational state, and the maximum value of the cross section for vibrational excitation, which occurs at about 3 eV, is two orders of magnitude below the collision cross section for momentum transfer in H_2.
(B) Although the operating regime of the nonequilibrium disk is just within the stable region with respect to ionization of the hydrogen, perturbations in the electron temperature could cause an ionization instability. The conduction processes in such fully ionized plasmas warrants experimental investigation.
(C) The electric fields experienced in the Full Ionization Case exceed previous experimental experience for insulating walls in MHD plasmas. Because the walls of the disk are not required to pass current except at the power take-off points, it is possible to increase the capability of the walls to sustain high voltage by transpiring cold hydrogen through the walls into the hot boundary layers of the disk. Analysis of the breakdown strengths in pure hydrogen suggests that the design wall stresses can be sustained with a considerable safety margin with such an approach.

(D) The reduction of the effective electrical conductivity and Hall parameter by the presence of plasma nonuniformities is expected to be small with full seed ionization. Nevertheless, this effect should be investigated in a small scale static conduction experiment.

The following subsections summarize the results of the plasma modeling effort.

3.1 The Ideal MHD Generator

Considering the MHD generator as an ideal expansion engine, one may obtain rough estimates for the performance potential and the geometry of the generator. The ideal MHD analysis makes the following assumptions:

(1) The working fluid is an ideal gas with a constant ratio of specific heats, γ.
(2) Friction and heat transfer are neglected.
(3) The local electrical conversion efficiency, η_e is constant in the generator.

With these assumptions one can derive expressions for the fraction of the inlet enthalpy extracted as electrical power, η_{enth}, for various design modes such as constant velocity, constant Mach number, constant temperature, and constant pressure. For reasons of plasma stability, the hydrogen disk operates with a relatively high inlet Mach number, 3.2. This approach favors designs that approach the impulse (constant pressure) mode. In fact, the approach taken in both the Full Ionization Case and the Reference Case is to design the generator to operate with constant gas temperature until the pressure in the channel falls to a prescribed level of approximately 0.14 atm. The outer part of the generator is designed as an impulse generator operating at the prescribed pressure of about 0.14 atm. This approach gives relatively constant wall separations along the radius of the disk.

Algebraic solutions for ideal MHD generator enthalpy extraction ratio and other ratios can be written for various assumed design approaches. In the impulse generator and the constant temperature generator, it is sufficient to specify the exit Mach number M_2 and electrical conversion efficiency η_e, since the enthalpy extraction is primarily by reduction of the kinetic energy of the working fluid. The algebraic solutions are the following:

(1) *Constant Temperature MHD Generator.*

$$\left(\eta_{\text{enth}}\right)_{\text{Const T}} = \frac{\frac{1}{2}(\gamma-1)(M_1^2 - M_2^2)}{1+\frac{1}{2}(\gamma-1)M_1^2} \tag{1}$$

$$\frac{p_2}{p_1} = \exp\left(-\gamma\left(\frac{1-\eta_e}{2\eta_e}\right)(M_1^2 - M_2^2)\right) \tag{2}$$

$$\frac{A_2}{A_1} = \frac{M_1}{M_2}\frac{p_1}{p_2} \tag{3}$$

(2) *Constant Pressure MHD Generator.*

$$\left(\eta_{\text{enth}}\right)_{\text{Const p}} = 1 - \frac{\left(1+\frac{1}{2}(\gamma-1)M_2^2\right)T_2}{\left(1+\frac{1}{2}(\gamma-1)M_1^2\right)T_1} \tag{4}$$

$$\frac{T_2}{T_1} = \frac{1+\frac{1}{2}(\gamma-1)(1-\eta_e)M_1^2}{1+\frac{1}{2}(\gamma-1)(1-\eta_e)M_2^2} \tag{5}$$

$$\frac{A_2}{A_1} = \frac{M_2}{M_1}\left(\frac{T_2}{T_1}\right) \tag{6}$$

Evaluating these expressions for typical values of the ratio of specific heats γ =1.3, the inlet Mach number M_1 =3.2, and the exit Mach number $M_2 = 1.2$ over a range of electrical conversion efficiencies η_e, it is seen in Table 6 that reasonable designs in either mode must have $\eta_e \approx$ 0.6–0.7.

Table 6. Ideal MHD Generators

Electrical Conversion Efficiency η_e=	0.4	0.5	0.6	0.7	0.8
Constant Temperature Generator					
T_2/T_1	1	1	1	1	1
p_2/p_1	0.0002	0.0033	0.0221	0.0862	0.2393
A_2/A_1	14,198	813	121	31	11
η_{enth}	52%	52%	52%	52%	52%
Constant Pressure Generator					
T_2/T_1	1.70	1.60	1.49	1.37	1.25
p_2/p_1	1	1	1	1	1
A_2/A_1	3.48	3.37	3.25	3.12	2.99
η_{enth}	18%	23%	29%	34%	40%

As expected, the ideal enthalpy extraction ratios are higher than but similar to the values achieved in the mixed-mode calculations of the Full Ionization Case and the Reference Case. The essence of the nonequilibrium MHD generator design problem

is to provide enough Joule dissipation to maintain the desired electron temperature elevation without demanding so much Joule dissipation as to cause an unsatisfactory electrical conversion efficiency.

3.1.1 The Ideal Disk Generator with Electron Non-equilibrium

It remains to specify the relationship between the loading, represented by the load factor K, and the electrical conversion efficiency in order to determine the ideal performance of the non-equilibrium MHD generator.

The ideal MHD generator dissipation power density required to maintain an electron temperature elevation of $(T_e - T)$ is, in its simplest form,

$$\widehat{P}_d = n_e \nu_e \delta_{\text{eff}} \frac{3}{2} k (T_e - T), \tag{7}$$

where n_e is the number density of electrons and $\nu_e = nQc_e$ is the total electron collision frequency in which $n = p/kT$, Q is the effective collision cross section for momentum transfer, k is the Boltzmann constant, $c_e = (8kT_e/\pi m_e)^{1/2}$ is the electron thermal velocity, and m_e is the electron rest mass.

The electron energy loss factor δ_{eff} is the average fraction of energy lost by an electron in a collision with another species of the working fluid (Ref. 13). It has the value $(2m_e/m_a)$ for perfectly elastic collisions of electrons with a species with molecular mass m_a. Species which allow transfer of energy to inelastic processes such as molecular vibrational and rotational modes have higher values of δ_{eff} and require correspondingly higher inputs of energy from Joule dissipation to maintain electron temperature elevation. Polyatomic molecules in combustion gases, such as H_2O and CO_2, have the highest values of δ_{eff}, while the noble gases have the lowest. For convenience the energy loss factor is often normalized to the elastic value: $\delta' \equiv \delta_{\text{eff}}/(2m_e/m_a)$.

The dissipated power density in an ideal MHD disk generator with conductivity σ, velocity U, magnetic field B, and load factor K is

$$\widehat{P}_d = \frac{J^2}{\sigma} = \sigma U^2 B^2 \left[\frac{1 + [\beta(1-K) - KS]^2}{(1+\beta^2)(1+S)^2} \right] \tag{8}$$

Note that in the limit of no swirl, the dissipation becomes

$$\widehat{P}_d(S=0) = \sigma U^2 B^2 \left[\frac{1 + \beta^2 (1-K)^2}{(1+\beta^2)} \right] \tag{9}$$

and in the limit of very large Hall parameter, the dissipation has the same form as the dissipation from a linear Faraday generator:

$$\widehat{P}_d(S=0;\beta=\infty)=\sigma U^2B^2(1-K)^2 \tag{10}$$

The generated power density in an ideal MHD disk generator is

$$\widehat{P}_g=\sigma U^2B^2K(1-K)\left[\frac{(\beta+S)^2}{(1+S^2)(1+\beta^2)}\right] \tag{11}$$

Again, note that in the limits of no swirl and large Hall parameters, the expression for power density has the same form as for a linear Faraday generator.

Finally, the electrical conversion efficiency in a disk generator is

$$\eta_e=\frac{K(1-K)(\beta+S)^2}{1+\beta^2(1-K)+KS^2} \tag{12}$$

Once again the disk equations take the same form as the linear Faraday equations in the limits of small swirl and large Hall parameter: as $S\rightarrow 0$ and $\beta\rightarrow\infty$, $\eta_e\rightarrow K$.

For simplicity, consider these limits in the following arguments (the virtual equality between K and η_e, especially in the Full Ionization Case, will become evident in the numerical results presented in the following sections). Then

$$\frac{\widehat{P}_d}{\widehat{P}_g}=\frac{(1-K)}{K}. \tag{13}$$

Suppose that, for a given set of gas conditions p and T corresponding to an expansion to Mach number M, an electron temperature T_e is required to produce an adequate electrical conductivity σ. Substituting into Eqs. (7) and (10) the following approximations for electrical conductivity

$$\sigma=\frac{n_ee^2}{m_e\nu_e} \tag{14}$$

and Hall parameter

$$\beta=\frac{eB}{m_e\nu_e}, \tag{15}$$

it is found that

$$\frac{T_e-T}{T}=\frac{\gamma}{3\delta'}(1-K)^2M^2\beta^2, \tag{16}$$

or, solving for K and eliminating β,

$$K_{max} \approx \eta_{e,max} \approx 1 - \frac{m_e}{e}\frac{nQc_e}{B}\left[\left(\frac{T_e - T}{T}\right)\frac{3\delta'}{\gamma M^2}\right]^{1/2}. \qquad (17)$$

Eq. (17) exhibits the effects that increase the efficiency of the ideal non-equilibrium MHD generator for a given elevation of the electron temperature over the gas temperature: low pressure (and hence low n), small collision cross sections Q, high magnetic field B, low energy loss factors δ', high specific heat ratios γ, and high Mach numbers M.

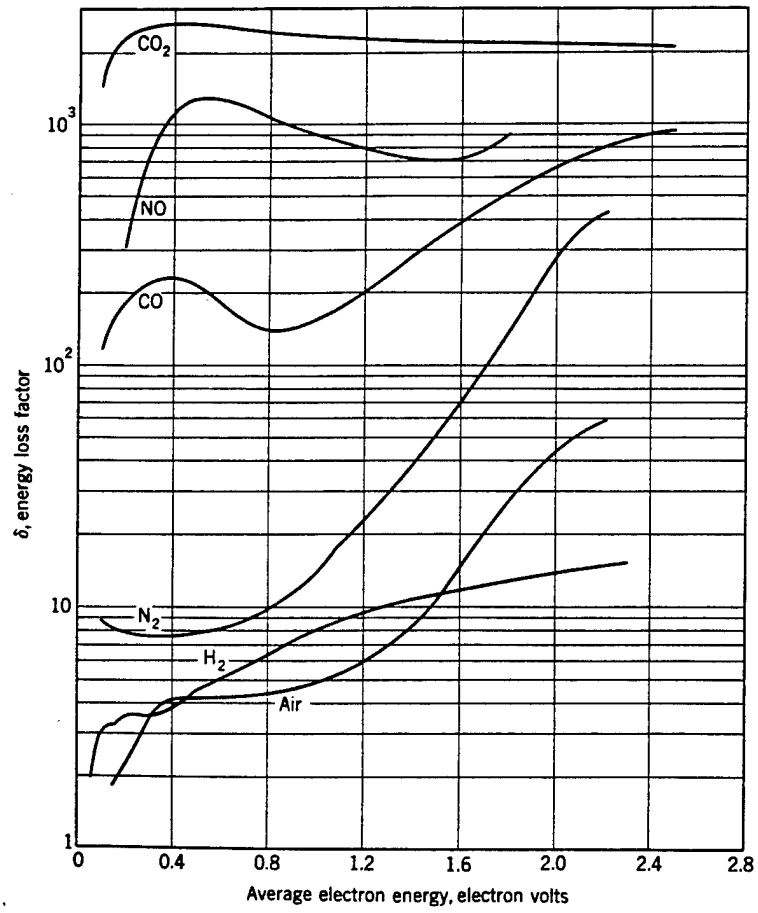

Fig. 17. Energy loss of electrons with maxwellian velocity distribution with various gases. (data compiled by H. Massey and J. D Craggs, *Handbuch der Physik*, 37/1, pp. 314–415, 1959). Figure reproduced from Ref. 14.

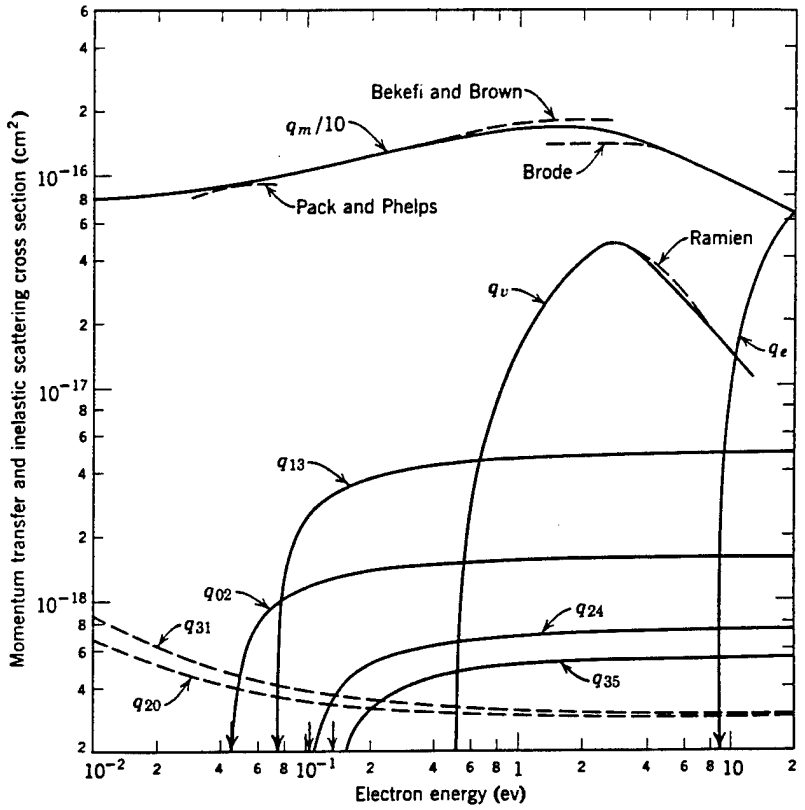

Fig. 18. Cross sections for H_2 as a function of electron energy: q_m is the momentum transfer cross section; q_{02}, q_{13}, q_{24}, q_{35}, q_{20}, and q_{31} are the cross sections for electron impact-induced transitions between the rotational states indicated by the subscripts times the fraction of the molecules in the initial state (first subscript) for the gas at 300 K; and q_v and q_e, are cross sections for the excitation of the first vibrational state and the electronic states. (Figure reproduced from Ref. 15).

Extensive measurements of δ' and Q for H_2 are available in the literature, and the data are for the most part very consistent. Figure 17, adapted from Ref. 14, illustrates typical values for hydrogen and other gases. Figure 18, adapted from Ref. 15, gives measurements of the electron collision cross section for momentum transfer as well as cross sections for other processes.

All of these data for δ' and Q were obtained in hydrogen essentially at room temperature. On the other hand, the vibrational and rotational temperatures of the hydrogen in the disk generator may be closer to the stagnation temperature. However, it is seen from Figure 18 that the cross section for vibrational excitation is two orders of magnitude smaller than the momentum transfer cross section. Therefore, the electron temperature should be only loosely coupled to the vibrational and rotational temperatures. The effective energy loss factor in a multicomponent, nonisothermal

plasma is given (Ref. 13) as

$$\delta_{\text{eff}} \equiv \nu_i^{-1} \sum_{\kappa} (2m_e/m_\kappa)\, \delta'_\kappa \tau_{e,\kappa}^{-1} \tag{18}$$

and since the contribution of each component or process κ is weighted by the collision time (inversely proportional to the cross section for that component or process), the effect of the vibrational temperature on the effective energy loss factor should not be large. Future experiments on helium/hydrogen mixtures would settle this question by making indirect measurements of the electron energy loss factor with a high stagnation temperature gas.

The Saha equation at temperature T_e may be used to compute the effect of elevated T_e on the electron number density n_e, since ionization by heavy particle impacts may be neglected. Therefore, if n_s is the number density of seed atoms (ion and neutral),

$$\frac{n_e^2}{n_s - n_e} = 2\,\frac{g_i}{g_n}\left(\frac{2\pi m_e k T_e}{h^2}\right)^{3/2} e^{-T_{\text{ref}}/T_e}, \tag{19}$$

The same equation applies to the ionization of the hydrogen gas by hot electrons. As is discussed in a later section, this effect places an upper bound on the electron temperature to avoid ionization instabilities involving the hydrogen working fluid.

3.1.2 The Full Ionization Case

The Westinghouse system code was employed to carry out a one-dimensional solutions of the disk MHD generator equations with friction and heat transfer presented in the previous section. Because of the constant temperature/constant pressure design with K values from 0.5 at the inlet (to "ignite" the electrons) to 0.7 in the main part of the disk, the enthalpy extraction values were similar to the ideal generator results shown above.

The plasma properties computed in this Full Ionization Case are shown in Table 7. No reduction formulas were applied to the property calculations to account for plasma nonuniformities, and this computation represents a case in which, because of the fully-ionized seed, the plasma properties vary only in r.

The highest experimentally observed effective Hall parameter has been on the order of $\beta \approx 14$. Such values have been seen in fully-ionized experiments in helium in Japan, for instance. Designs with β_{eff} values of 15 or higher may be optimistic, but, as will be seen in the following section, the performance and weight penalty for inclusion of the effects of moderate nonuniformities is not severe.

Table 7. Plasma Properties at Inlet, Middle, and Exit of the Full Ionization Case

r (m)	0.2	0.4	0.6
T (K)	1129	1255	1488
p (bar)	0.300	0.1390	0.1390
U_r (m/s)	7976	6558	4486
U_θ (m/s)	-28	-271	-473
M	3.168	2.481	1.575
B (T)	4.0	3.5	3.5
T_e (K)	7305	7549	6645
n_e (m^{-3})	2.87×10^{19}	1.20×10^{19}	1.01×10^{19}
σ_{eff} (S/m)	7.009	6.895	7.339
β_{eff}	6.069	12.527	15.805
J_r (A/cm^2)	1.92	0.90	0.52
J_θ (A/cm^2)	10.69	4.55	3.33
E_r (kV/m)	89.70	80.41	68.98
K	0.536	0.719	0.720
η_e	0.506	0.699	0.700
$\vec{J}\cdot\vec{E}$ (MW/m^3)	1725	724	358
$\vec{J}\cdot\vec{E}'$ (MW/m^3)	1683	312	155

3.2 Non-ideal Effects in the Hydrogen Non-Equilibrium MHD Generator

Several effects would reduce the performance of a non-equilibrium hydrogen MHD generator from the ideal values shown in Table 6. Evaluation of these effects is possible with the fully coupled, three-dimensional, time-dependent solutions of the equations for the gas dynamics, plasma state, and electrodynamic fields in the generator which have been developed at STD Research Corporation (Ref. 16). In the present study a number of critical phenomena were isolated and evaluated separately based on the design operating regimes. In future analysis these models will be available to carry out more detailed evaluation of these phenomena.

Many non-ideal processes may limit the performance of the non-equilibrium hydrogen generator. In the following discussion we will estimate the effect of the following important processes: (1) high magnetic Reynolds number effects, (2) ion slip, and (3) plasma fluctuations associated with electron energy relaxation, recombination effects, and plasma instabilities.

3.2.1 Effect of Magnetic Reynolds Number

The magnetic Reynolds number is

$$R_m \equiv \mu_0 \sigma U L. \tag{20}$$

For values of R_m greater than unity, performance tends to saturate because of the exclusion of the magnetic field from the core of the flow (Ref. 17).

Based on the mid-channel conditions in the Full Ionization Case above, we find $R_m \approx 0.05$, and magnetic Reynolds number effects can be safely neglected in the Hydrogen disk generator, at least at the seed fractions considered in the present design.

3.2.2 Effect of Ion Slip

In the first approximation to the general Ohm's law formulation, the effects of current transport by ions instead of electrons appears as a simple correction to the electrical conductivity and Hall parameter (Ref. 18):

$$\frac{\sigma'}{\sigma} = \frac{\beta'}{\beta} = \frac{1}{1 + \beta_e \beta_i}, \tag{21}$$

where β_e and β_i are the electron and ion Hall parameters. Typically, $\beta_e/\beta_i \approx 10^2$–$10^5$, and ion slip accounts for a 0.01% correction to the conductivity and Hall parameter.

3.2.3 Electron Energy Relaxation Effects and Recombination Effects

Analysis of the electron energy equation leads to the following expression for the characteristic length for electron energy relation (Ref. 19):

$$L_E = \frac{4}{3} \frac{U}{\nu_e \delta_{\text{eff}} \gamma_e} \left[\ln \left(1 + \frac{\gamma_e T_e}{T_e - T_g} \right) - \gamma_e \right], \tag{22}$$

where

$$\gamma_e \equiv 2kT_g/\epsilon_i. \tag{23}$$

Evaluating this electron energy relaxation length for the ideal hydrogen MHD generator, we find L_E =0.1–0.3mm for the conditions of the Full Ionization Case.

Ref. 19 also gives the expression for the characteristic length for radiative/collisional recombination:

$$L_R = 0.433U/\left[\hat{r}(T_e)n_{e,o}^2\right] \tag{24}$$

where $\hat{r}(T_e)$ is the three-body recombination coefficient. For the conditions of the Full Ionization Case L_R ranges from 0.09–2.6 mm

These short energy relaxation and recombination lengths mean that convective effects will not be important in these devices and that the local properties will be determined by the local electron temperature, rather than the upstream history of the flow.

The application of the two-temperature model for electron nonequilibrium requires that the recombination process proceed more rapidly than the energy relaxation process. Since they are comparable in the present designs, the operating conditions may be at the lower limit for seed fraction. This suggests that a small increase in seed fraction and a slight reduction in the electron temperature would increase plasma stability.

3.2.4 Insulator Wall Breakdown Prevention

An analysis was carried out of the likely characteristics of the insulator wall boundary layer characteristics. It is well known that supersonic flows may exhibit temperature overshoots in the boundary layers. That the boundary layer temperature can exceed the core temperature is a consequence of the recovery of stagnation pressure as the gas is slowed at the wall. Preliminary estimates of the temperature overshoot in boundary layers of the Reference Case amount to a few hundred degrees Kelvin. Since, according to Eq. (17), the parameter $(T_e - T)$ is crucial to the local performance of the nonequilibrium disk, a local variation in T could lead to a local, high conductivity channel at the sidewalls. Since MHD is a volume process, it is possible that a great deal of the power generated in the bulk of the plasma could be channeled through such a conducting path.

To minimize this problem, transpiration cooling of the insulating walls could be employed to build up a film of relatively cool, relatively pure hydrogen at the walls. The "hydrogen wall" will have these advantages that could justify some additional complexity: (1) local hot spots in the gas temperature profiles will be controlled and minimized, (2) the heat load to the insulating walls will be reduced, and (3) seed deposits on the insulating walls may be reduced. Because of the highly supersonic flow in the core, to avoid shock losses, it will be necessary to introduce the wall hydrogen at low velocity normal to the flow.

The disk geometry is inherently less susceptible to insulator breakdown because, except at the power take-off points, current is not forced to penetrate the cold wall boundary layers, a process which tends to create arcs and other temperature disturbances in the boundary layers. Also, because the current is not forced

repeatedly to penetrate the boundary layer, the tendency to concentrate equipotentials at conductor/insulator boundaries is reduced. The formation of a cool, pure layer of hydrogen over the insulating wall could have the advantage that any field concentration that might build up on the insulator wall will be shielded from the core by a fairly good insulating medium, hydrogen.

Louis has reported that radial electric fields up to 30 kV/m were observed in shock-driven disk generators. This value is well below the design electric fields in the full scale designs, but it is nearly an order of magnitude higher than in most linear MHD generators. A Paschen-type analysis was carried out for pure hydrogen under typical operating conditions of the Reference Case. The results of this analysis suggested that field strengths up to 300 kV/m could be sustained. This will be an ample margin of safety against insulator wall breakdown.

3.2.5 Plasma Stability Regimes

Figure 19 superimposes the regimes of stable plasma operation for cesium-seeded hydrogen and helium. This stability map covers likely ranges of seed fraction and electron temperature and displays the values which may lead to instabilities of the following kind:

(1) Cesium-related electrothermal instability. The left-hand boundaries are defined as the loci of conditions in which the seed is 99% ionized.

(2) Hydrogen-related electrothermal instability. The right hand boundaries are defined as the loci of conditions in which the electron number density from hydrogen or helium ionization is equal to the electron number density from seed ionization.

(3) Static instability (see Ref. 21). The upper boundaries are defined as the loci of points at which Coulomb collisions occur as frequently as electron/neutral collisions.

It was noted that the stable operating regime of the Hydrogen disk is narrower than for helium because of hydrogen's lower ionization potential. The stable operating regimes should be investigated experimentally in future research in a static conduction test cell that will simulate a wide range of operating conditions with realistic hydrogen/cesium working fluids.

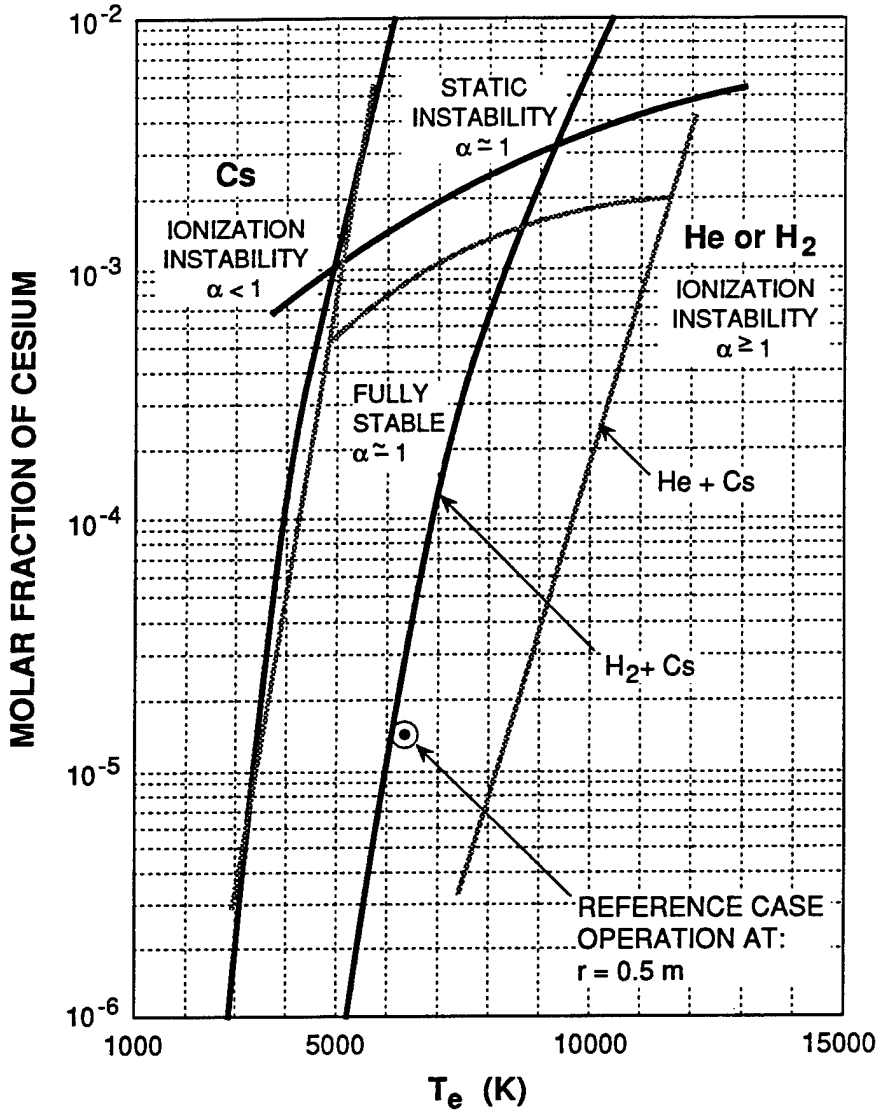

Fig. 19. Stability map for the operating conditions of the Reference Case at $r = 0.5$ m (black lines). Also shown for comparison is the stability map for cesium-seeded helium working fluids (grey lines).

3.2.6 Effects of Nonuniformities and Fluctuations

Experiments in the linear and disk generators with electron nonequilibrium have confirmed that the plasma may be unstable for conditions of practical interest and that the electron temperature may not be uniform when the seed is not fully ionized, when the plasma is Coulomb-dominated, or when the working fluid begins to ionize, as described in the previous sections. These effects were predicted by Velikhov (Ref. 20) and Kerrebrock (Ref. 21). It was also shown (Refs. 22 and 23) that the effective

plasma properties σ_{eff} and β_{eff} can be described by a reduction formula so that

$$\frac{\sigma_{\text{eff}}}{\langle\sigma\rangle} = \frac{\beta_{\text{eff}}}{\langle\beta\rangle} = \frac{1 + 3\langle\beta\rangle a}{1 + \langle\beta\rangle^2 a} \tag{25}$$

where the nonuniformity parameter is defined as

$$a \equiv \left(\frac{1 - \langle\alpha\rangle}{\langle\alpha\rangle}\right)^2 \tag{26}$$

for high degrees of ionization α >0.5. The empirical coefficient 3 in the numerator of Eq. (25) comes from the work of Klepeis and Louis (Refs. 24 and 25), who studied the performance of a disk generator with nitrogen and found that the value 3 more accurately explained the measured β_{eff}. They suggested that the difference between the atomic and molecular working fluids results from the energy exchange between the electrons and the vibrational levels of diatomic gases such as N_2 and causes the coefficient to exceed the values between 1 and 2 found for argon and helium.

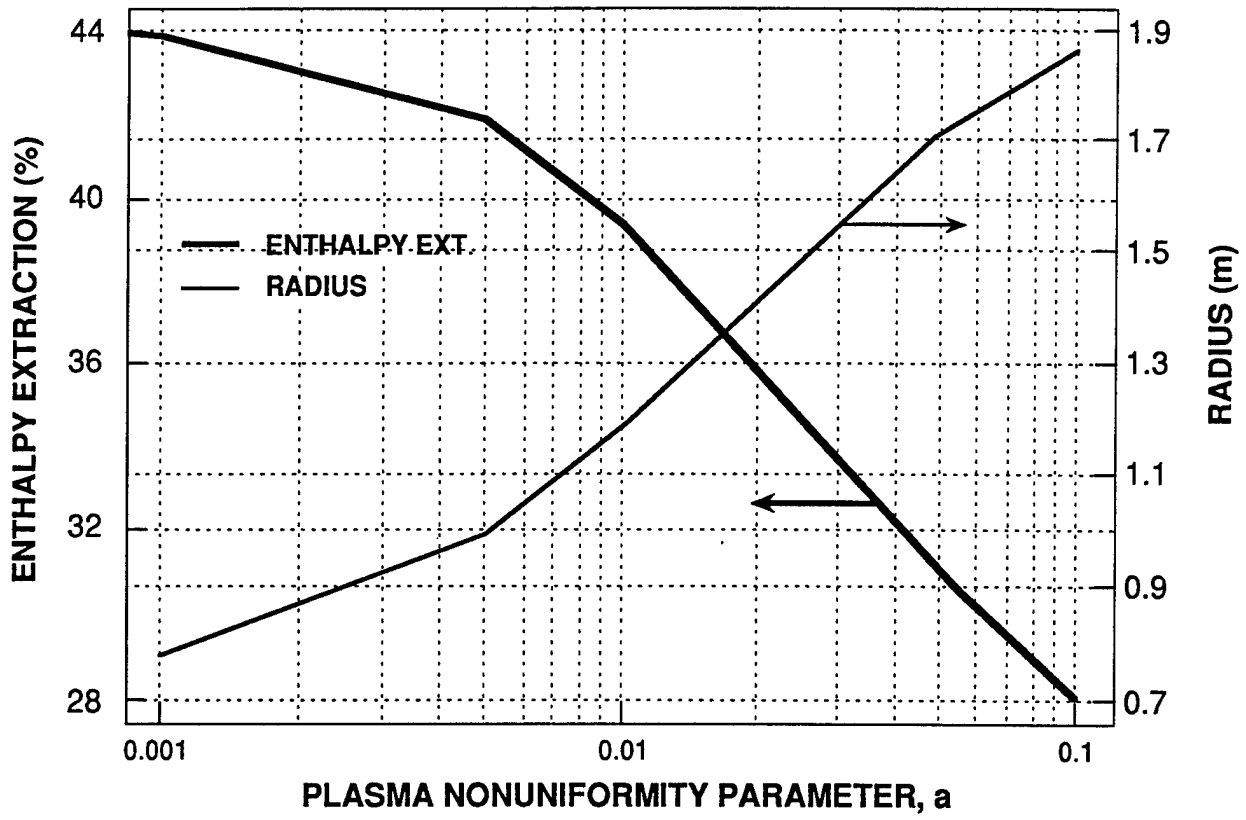

Fig. 20. Enthalpy extraction and disk exit radius as a function of the plasma nonuniformity parameter a.

The present modelling effort utilized Eq. (25) and surveyed the performance of the disk generator for various degrees of ionization $\langle\alpha\rangle$. As expected, the reduction in conductivity and Hall parameter reduced the interaction and produced somewhat larger, somewhat less efficient generators, as shown in Figure 20, which repeats the particularly important Figure 4 for the convenience of the reader.

Table 8. Plasma Properties at Inlet, Middle, and Exit of the Reference Case

r (m)	0.25	0.5	0.75
T (K)	1129	1273	1483
p (bar)	0.223	0.142	0.142
U_r (m/s)	7820	6498	4858
U_θ (m/s)	-78	-365	-605
M	3.106	2.444	1.712
B (T)	3.5	3.5	3.5
T_e (K)	7739	6561	5717
n_e (m^{-3})	2.14×10^{19}	1.21×10^{19}	1.04×10^{19}
σ_{eff} (S/m)	6.060	4.695	4.149
β_{eff}	6.181	8.469	8.720
J_r (A/cm^2)	1.40	0.90	0.58
J_θ (A/cm^2)	7.95	3.09	2.04
E_r (kV/m)	78.51	52.50	39.36
K	0.535	0.726	0.731
η_e	0.505	0.681	0.677
$\vec{J}\cdot\vec{E}$ (MW/m^3)	1097	470	226
$\vec{J}\cdot\vec{E}'$ (MW/m^3)	1075	220	108

3.2.7 The Reference Case

The Reference Case was chosen on the basis of a target plasma nonuniformity parameter $a = 0.005$. The plasma properties for the Reference Case are given in Table 8.

CHAPTER 4

ENGINEERING EXPERIMENT DEFINITION

The systems analysis and modeling activities have demonstrated the feasibility and attractiveness of the hydrogen-driven MHD disk generator. The results of the analyses performed to date now warrant the experimental demonstration of feasibility to emphasize experimental verification of the analytical results obtained in this study. New experimental data will be incorporated into the analytical models and a final design of a full-scale generator will be the final objective of the project. The design of the engineering experiments that will demonstrate feasibility of the hydrogen-driven MHD disk generator is guided by the following principles:

(1) Cost At this stage the construction of a full-scale working MHD generator driven by 5 kg/s per second of hydrogen is probably not justified. The primary limitation is on development of the full-scale heat source. Obviously, there are no working NERVA engines. Electrically-heated reactors would require the output of a small power plant to operate. Instead, we have chosen to design experiments at about 1/1000 power that will verify the operation conditions of the full scale generator with respect to critical issues that are identified in this report.

(2) Realistic Working Fluid Simulation Various options were considered for the heat source for the working fluid in the engineering experiments. The most realistic heat source is a simulation of the NERVA reactor heat transfer process from graphite to hydrogen. Apparatus from earlier experiments could be utilized to simulate the working fluid produced by a NERVA to carry out low flow rate, "static" conduction tests that will establish the stability of current conduction under the conditions of the full scale disk generator. A graphite "resistojet" heater that will produce a hydrogen flow rate of 5 to 10 g/s could also drive a subscale disk generator. This approach would prove that stable conduction *and* power generation can occur in the disk generator configuration.

(3) Applicability To Full-scale MHD Generator Performance Basic plasma physics data and scaling information will be obtained in the large disk experiment with shock-heated mixtures of hydrogen and helium or hydrogen and argon in one of the disk generator facilities in Japan. This experiment, while it will lack the working fluid realism of the other two experiments, will nevertheless provide basic plasma physics parameters relevant to the modeling of these devices. The demonstration of the effects of hydrogen addition upon the performance of the fully-ionized He/Cs disk generator will provide insights to the following issues: (1) The dependence of hydrogen ionization instability on the electron temperatures; (2) the dependence of the hydrogen energy loss factor on the stagnation temperature of the working fluid as well as the electron temperature; and (3) the effects of hydrogen addition on the electron collision cross section for momentum transfer or the effective electrical conductivity of the plasma.

The following sections define the experiments that will be carried out to achieve these objectives.

4.1 Static Conduction and Insulating Wall Demonstration Experiment

Extensive and systematic investigations of plasma conduction stability in non-equilibrium plasmas were carried out in the early 1960's at MIT under the direction of Professor J. Kerrebrock. In Kerrebrock's experiments (Ref. 21), a simple counterflow heat exchanger powered by a nitrogen arcjet apparatus was used to produce a seeded working fluid for an electrode array through which passed current. The apparatus had considerable flexibility in the important operating parameters of gas temperature, gas composition, seed fraction and electron temperature. Unfortunately, none of these experiments utilized hydrogen, and none were carried out in the low-seed-fraction, fully ionized regime.

During the first year of the next stage of the project, a similar apparatus will be constructed to carry out the tests with hydrogen in the STD Research Corporation vacuum test facility. Because of the low flow velocities expected in the test cell, back pressure control will be necessary in order to simulate the operating conditions of disk generator over its entire length in which pressures vary from slightly less than 1 atmosphere to slightly more than 0.1 atmosphere. The other significant modifications to the Kerrebrock apparatus is that the counterflow heat exchanger will be constructed entirely from graphite instead the tantalum tubing that was utilized at MIT. This change will allow the simulation of heating in a NERVA reactor, which could introduce carbon species that would be relevant to the conduction phenomena. If time and resources allow, this possibility will be checked in two ways: (1) The exhaust from the test section will be tested with a gas chromatograph in order to identify carbon species that may be formed in the heat transfer process and (2) the experiments carried out with graphite heat exchanger will be reproduced under one set of operating conditions with a tantalum tube in place of the graphite in order to identify any differences in the conduction process when the possibility of carbon contamination is eliminated. The other change in the experimental apparatus will be the use of argon in place of nitrogen in the arcjet heat source for the heat exchanger. This will avoid the formation of CN-related species that could form if the graphite heat exchanger were exposed to nitrogen at several thousand Kelvins. Although it is not expected that such an effect would pose a health hazard, nevertheless, the possibility exists, and it will be less troublesome to conform with OSHA requirements if the heat exchanger working fluid is an inert gas.

The construction of this low-cost, small-scale experimental facility would enable future efforts to address two critical issues identified in this study. The first issue is the possibility of insulator wall breakdown in the disk generator. Because the full-scale disk design could incorporate pure hydrogen transpiration on the insulator walls to

provide a low-conductance thermal and electrical insulation on the walls, and because the analysis performed in this study indicates that much higher electric fields can be sustained by this technique, the ability of the insulating wall to sustain such electric fields can be demonstrated in this facility if sufficiently high voltages are applied across pure hydrogen flows. The first series of tests to be carried out in the static conduction test facility will be carried out without seed. An extensive survey of the breakdown characteristics of the graphite-heated hydrogen will be conducted before the heater and the remainder of the test cell are contaminated with Cs seed. Following the insulating wall voltage standoff demonstration, the seeding subsystem will be introduced and a series of tests will be carried out to demonstrate stable conduction throughout the expected operating envelope of the MHD disk generator driven by hydrogen.

4.1.1 Plasma Breakdown Tests

The analysis in Section 3.2.4 indicates that the breakdown strength of hydrogen is approximately 300 kV/m. In a 1-inch test cell, this breakdown strength will require voltages of approximately 10 kV. Such voltages are readily available in capacitor banks available at STD Research Corporation. The plasma breakdown tests will be carried with the high-voltage provided by capacitors. Series resistance and inductance will prevent the current from rising above a critical level, so that destructive arcs will not be permitted to form. The applied voltage will be regulated by means of a voltage divider network.

4.1.2 Plasma Stability Tests

When all of the data on hydrogen breakdown has been obtained, the seed system will be connected to the experiment. The conduction through hot hydrogen over the entire range operating conditions of the disk generator design will be surveyed for stability and conductivity. The parameters that will be varied are the following: Seed fraction, current density, gas temperature (as measured by a pyrometer in the heat exchanger), electron temperature (as measured by the Cs D-line reversal technique), and gas pressure. The results of these experiments will be correlated with the model calculations and a map of the likely stable operating regimes of the disk generator will be prepared. This map will be used to finalize the design conditions for the full-scale disk generator as well as for the sub-scale disk generator. The tests with the static conduction facility can be completed in one year, and information obtained in these experiments will be used to guide the tests of the sub-scale disk generator.

4.2 Hydrogen/Noble Gas Shock Tube Disk Generator Experiment

Simultaneously with the experiments on the static conduction and the subscale disk generator, experiments will be conducted with cesium-seeded noble gas/hydrogen mixtures. This work will be an extension of the previous fully-ionized MHD Disk generator studies in Japan. The tests, which will be carried out on a no-cost basis, will provide information on the electron energy loss factors and on the effect of hydrogen on the performance of a shock-driven helium/cesium disk generator.

4.3 Test of Experimental Disk Generator

Having established the map of stable operating regimes in static conduction tests, and having measured basic plasma parameters to guide the modeling of these plasmas, the final step in the experimental work will be to apply these to an actual disk generator experiment at small scale.

The design of the sub-scale disk generator experiment is constrained by the following factors: (1) The limitations of electrical power that can be applied to heat hydrogen. STD Research Corporation laboratory power rating is approximately 1 megawatt. Up to half of this power rating would heat hydrogen for the purpose of testing a sub-scale disk generator. The 500 kW of electrical heating will provide hydrogen flow rates of up to 10 g/s in the disk generator at the highest temperature operating condition. (2) The scale of the experiment will be constrained by the dimensions of the inlet of the disk generator. Therefore, it will not be possible to simulate in one experiment the entire operating regime of a 1 m long experiment. For example, if the inlet of the disk were less than 1 cm tall (distance between top and bottom insulating wall) and the disk generator were a realistic radius (for example, 0.8 m), the surface to volume ratio of such a disk generator would be entirely inappropriate for realistic power generation experiments. Therefore, a geometry could be utilized which matches the proportions of the full-scale disk but which will operate at a variety of conditions in separate experiments to simulate, piecemeal, the entire operating envelope of the full-scale disk. A variable throat section will be easily modified to provide inlet flows of a range of Mach numbers spanning the operation of the full-scale disk.

In keeping with the philosophy of utilizing realistic heat sources for the seeded hydrogen plasma working fluid, we propose to utilize a graphite "resistojet" design for the hydrogen heater. This will carry forward the experiments in the static conduction facility and provide the opportunity of studying the effect of possible contamination by carbon species in the working fluid. The "resistojet" technology is fairly well established, although typical units that have been developed at somewhat smaller scales than we propose, due to limitations of power suppliers in space, which is the primary application of "resistojet" technology. We have developed an efficient design

which should convert more than 90% of the dissipated heat in the graphite into hydrogen enthalpy.

The seeding systems to be used in the static conduction tests, in the first year, will have the capability of providing the seed for the MHD disk generator experiments as well. The flow rate of seed into the working fluid can be manipulated over two orders of magnitude by the choice of the heating medium for the seed. For example, if one uses liquid tin as the heating medium, one obtains a flow rate of Cs atoms two orders of magnitude less than if one uses liquid zinc. Furthermore, the seed fractions can be varied by varying the dilution of the seed with hydrogen and bypassing some of the resulting fluid.

A number of options were considered to provide the 3.5–4 T magnetic field for the disk generator experiment. These included the following: (1) An existing superconducting magnet constructed for disk generator tests of approximately the scale we propose, (2) an existing water-cooled, steady-state air core magnet available at the MIT Magnet Laboratory, and (3) an inexpensive, uncooled, normal magnet to be operated in the pulsed mode. Because of the additional complication and expense that cooling systems would introduce, and because the primary objective of demonstrating stable power generation can be met without requiring long duration operation, the third option was selected. The pulsed magnet parameters are described in Section 6.3.4 below. The magnet will be driven by a capacitor bank which will provide magnetic field pulses up to 4 T for durations of 100 ms. This represents tens of thousands of flow times and will give a picture of the MHD generator performance over the entire span of possible magnetic fields.

A comprehensive test program has been planned to provide demonstration of power generation at front-end, mid-channel, and exit operating conditions of the full-scale disk. The nominal operating conditions are summarized in Table 9.

Table 9. Nominal Operating Conditions of the Subscale Disk Generator Experiment

σ_{eff}	6.2	S/m
β_{eff}	11	
J_r	0.8	A/cm^2
J_θ	3.8	A/cm^2
$E_{r,max}$	40	kV/m
$\vec{J} \cdot \vec{E}$	150	MW/m^2
I	30	A
V	1	kV
P	30	kW

CHAPTER 5

ENGINEERING EXPERIMENT DESIGN

Preliminary designs of each of the major components of recommended future experiments are reported in this chapter. These include the major components of the static induction experiment: The cesium evaporator, the hydrogen heater, and the test cell. In addition, we have considered the design of the cesium condenser and exhaust system from the point of view of safety. It has also been verified that the hydrogen flow rates contemplated for both the static conduction experiment and the disk generator experiment can be managed by the vacuum tank pumps on the existing vacuum system. The safety of the facility will be assured by an over-specified exhaust system which will dilute the hydrogen in the exhaust to levels well below the explosion limits for hydrogen in air. Other aspects of static induction experiment design are discussed below.

The parameters of the experimental disk generator have been established to accommodate existing facility limitations. The hydrogen "resistojet" design is based on existing capabilities at the STD Research Corporation Laboratory. The generator design is derived from the operating envelope of the systems calculations that have been performed to date. If additional theoretical work indicates that other operating regimes are more suitable, it will be easy to modify the contours of the disk generator design. The disk generator is constructed of inexpensive insulator materials that can be machined to high tolerance. Essentially, steady state operation of the resistojet/jet generator system will be possible by minimal amounts of water cooling of the outer surfaces of the generator and resistojet heat source. This water cooling can easily be provided by existing laboratory water cooling systems.

The following subsections describe the design parameters of the major components of each experiment.

5.1 Static Conduction Experiment

5.1.1 Cesium Evaporator

Table 10 summarizes the vaporization characteristics of Cesium as a function of temperature in liquid melts of three candidate metals: tin, lead and zinc.

It is evident that a two order of magnitude variation in the evaporation rate of cesium can be obtained simply by selecting the proper melt material. In a typical experiment at

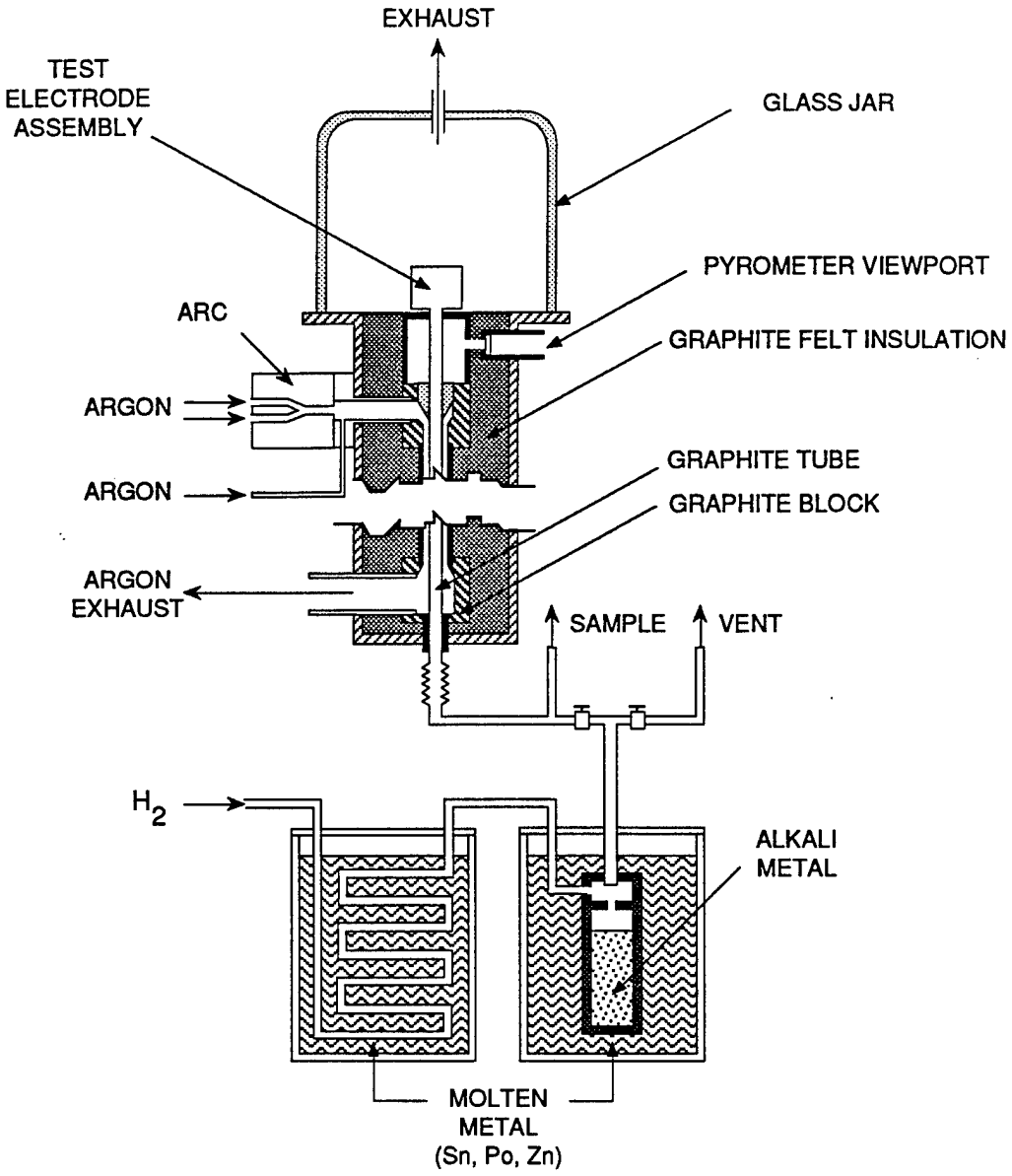

Fig. 21. Static conduction test facility for measuring breakdown and plasma stability in pure and weakly seeded hydrogen heated in a graphite heat exchanger. The primary heat source is an existing plasma torch operating with argon. Tests will be carried out in an existing vacuum chamber to simulate operation of the disk generator down to pressures of 0.1 bar.

the nominal flow rate of hydrogen (0.3 g/s), the required flow rate of cesium would be approximately 3 micrograms per second on cesium. Such low flow rates of cesium could be obtained at even lower working temperatures of the cesium. It would not be necessary in that case to use liquid metal in the melt, but rather an oil such as silicone oil could be used in place of the liquid metal to raise the cesium to temperatures of

Table 10. Vaporization Characteristics of cesium for Various Bath Temperatures

Bath Material	Melting Temperature (K)	Cesium Vapor Pressure (torr)	Cesium Evaporation Rate (atom/cm^2·s)
Oil	400	0.00276	4.20×10^{17}
Sn	504	0.2608	3.54×10^{19}
Pb	600	4.13	5.14×10^{20}
Zn	692	28.38	3.29×10^{21}

100–200 C. Small variations in the cesium flow rate then could be maintained by simply adjusting the temperature of the bath.

5.1.2 Hydrogen Heater

The enthalpy of hydrogen is approximately 47 MJ/kg at 2900 K. The enthalpy available in the arcjet heater is approximately 30 kilowatts. Therefore, flow rates up to 0.6 g/s of hydrogen can be heated to the full stagnation enthalpy of 47 MJ/kg. In the static conduction tests it is likely that much lower temperatures will be carried out, since the effect of high velocity on the static temperature of the gas will not be present. Therefore, tests with static temperatures as low to 1200 to 1300 K will be of interest in the electron non-equilibrium conduction tests. In these cases, the flow rate of hydrogen in the test cell can be increased to approximately 1.2 g/s or higher. Flow rates in this range will be passed through the graphite tube in the counterflow heat exchanger. The existing vacuum tank facility has provisions for a door-mounted arcjet in place. Therefore, the counterflow heat exchange tube for the hydrogen heater will be mounted on the inside of the vacuum chamber door. The exhaust from the argon arcjet will be ducted around the experimental apparatus and passed through a heat exchanger to remove the residual enthalpy before the argon is expelled from the chamber by the vacuum pumps. A relatively high flow rate of argon (20 g/s) will dilute the hydrogen effluent in the vacuum chamber significantly before the gas is collected by the vacuum pumps. This will reduce the requirements of dilution of the hydrogen in the exhaust system. The nominal design parameters of the hydrogen heater system are given in Table 11.

Table 11. Graphite Tube Heat Exchanger Operating Parameters

Tube O.D	1	cm
Tube I.D.	0.7	cm
Tube Length	20	cm
Argon Temperature	3100	K
Working Pressure	1	bar
Maximum Gas Temperature	2900	K
Maximum Graphite Temperature	3100	K
Mass Flow Rate	0.3–1	g/s
Power	30	kW
Start Time	20	s

5.1.3 Static Conduction Test Cell

The nominal design of the static conduction test cell will employ graphite electrodes separated by boron nitride insulators. The test cell will have a square cross section with a cross section dimension of approximately 1 cm. One set of opposing walls will be conductors consisting of graphite electrodes. The other set of opposing walls will be constructed of insulating material, boron nitride. Voltage will be applied across the conductors, first in a pure hydrogen working fluid to test the breakdown strength in the boundary layers of the disk and secondly, in a seeded hydrogen plasma to measure the conduction stability of the working fluid. Back pressures in the test cell would be approximately 0.1 atm. There will be "choke point" in the exhaust from the test cell compartment, to prevent argon or other background gases from contaminating the experiment.

5.2 Hydrogen/Noble Gas Shock Tube Disk Generator Experiment

As noted previously, Japanese investigators will be carrying out tests in their shock tube and blow down facilities. The exact design of these experiments will be worked out with the principal investigators at the Tokyo Institute of Technology in the next phase of the project.

5.3 Test of Experimental Disk Generator

The apparatus for the engineering test of the disk generator will consist of a novel "resistojet" hydrogen heater, a disk MHD generator, a pulsed magnet, all mounted in a vacuum chamber test cell. The following section describes the nominal design parameters of the test equipment.

5.3.1 Hydrogen Resistojet Design

The graphite heater is the heart of the resistojet design. It is a one-pass tube heater which is resistively heated by passage of DC current through the graphite. Graphite cross-section design is chosen to match the characteristics of the welding rectifier bank available at STD Research Corporation for running its arcs. Sufficient heat transfer surface area is provided to enable the ultimate of 2900 K to be obtained in the hydrogen. Nominal design parameters of the hydrogen heater are given in Table 12.

Table 12. Graphite "Resistojet" Operating Parameters

Graphite width	13	cm
Passage Diameter	0.7	cm
No. of Passages	217	
Graphite Height	1.5	m
Graphite Resistance	15	mΩ
Working Pressure	20	bar
Maximum Gas Temperature	2900	K
Maximum Graphite Temperature	3100	K
Mass Flow Rate	5–10	g/s
Power	200–400	kW
Start Time	120	s

5.3.2 High Voltage Source

The high voltage source will be a regulated power supply consisting of high voltage capacitors fed through high resistance to limit the current and arc breakdown potential in the system.

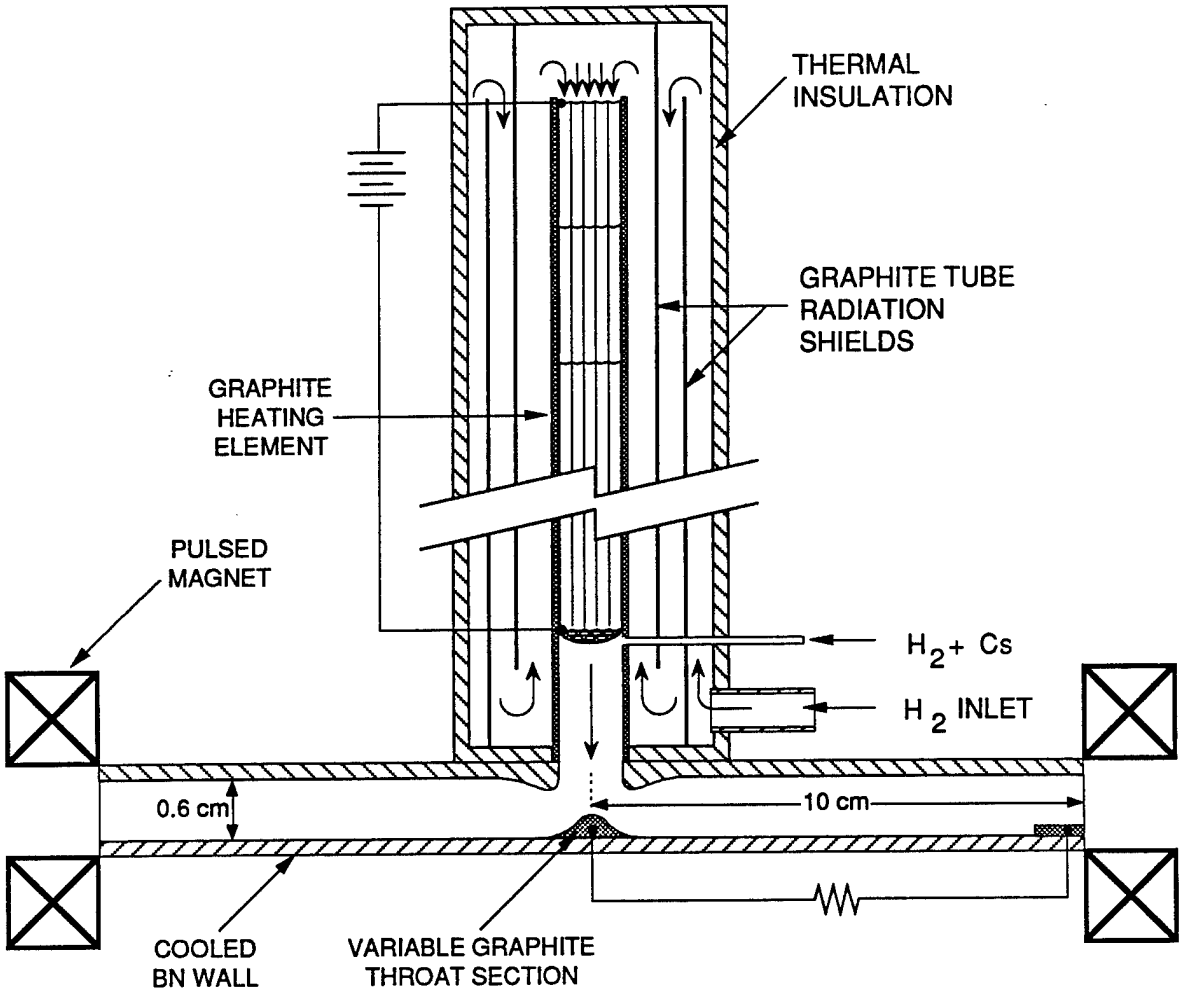

Fig. 22. Schematic diagram of 5–10 g/s disk generator experiment. The heat source is a resistively heated graphite "resistojet" to simulate the graphite nuclear heat source in the full scale system. The seed is introduced in a hydrogen stream produced by the equipment developed for the static conduction tests.

5.3.3 Preliminary Generator Design

Nominal design point for the MHD disk generator is based on a flow rate of 10 g/s. Table 13 gives the principal design parameters of the MHD generator design. The nominal Mach number will be 2, and with the inclusion of various throat inserts, the Mach number can be increased or decreased as desired.

Table 13. MHD Disk Generator Nominal Design Parameters

Disk Radius	10	cm
Disk Separation	0.62	cm
Throat Area	0.47	cm^2
Static Temperature	1813	K
Velocity	6123	m/s
Stagnation Temperature	2900	K
Stagnation Pressure	20	bar
Mass Flow Rate	10	g/s
Power	30	kW

5.3.4 Pulsed Magnet

The nominal design of the pulsed magnet is based on a magnetic field of 3.5 T. The inductance of the magnet is approximately of 1.3 H. To obtain a time constant of 100 ms, a capacitance of 7.6 mF is required. The total energy stored in the magnet can be estimated from the volume and magnetic field. The energy required is approximately 4kJ. This energy can easily be stored in 3 of the existing capacitors. Given the inductance and energy, the current can be computed from the formula $E = \frac{1}{2}LI^2$. The peak current is 100 A. In the worst case, the entire 4 kJ of energy would be dissipated in the magnet coils. The estimated temperature rise in the conductors, if they are one-inch in cross section, would be approximately 3°C.

5.3.5 Vacuum Tank Test Facility

Figure 23 is a photograph of the existing vacuum tank facility in which the static conduction and subscale disk generator engineering tests will be carried out. The existing facility will be modified to permit the addition of hydrogen, coolant for the cesium condenser, electrical through fitting, and other minor modifications. Otherwise

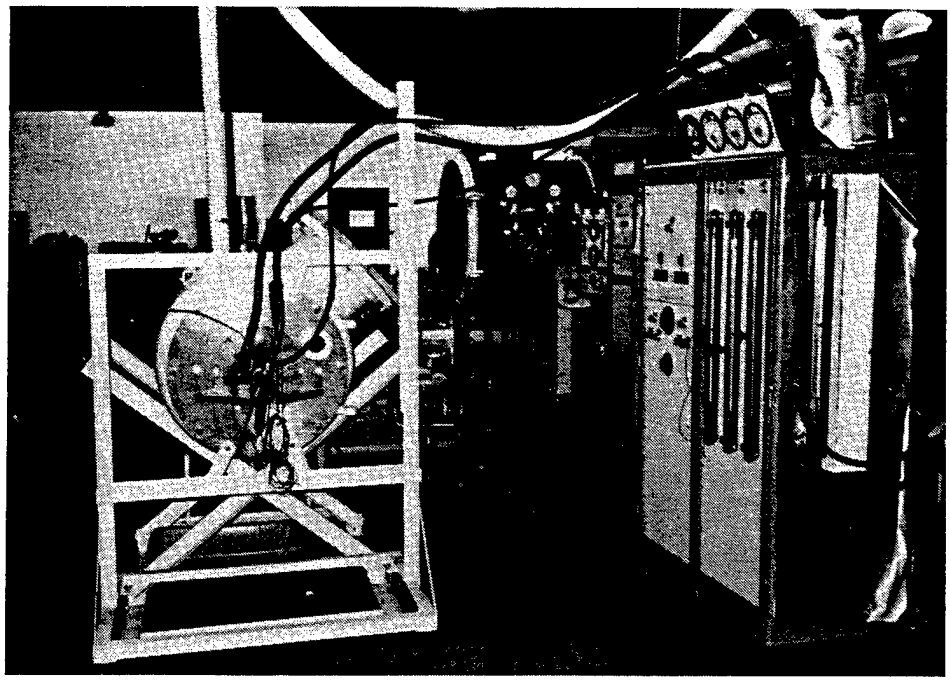

Fig. 23. Photograph of Vacuum Test Facility at STD Research Corporation, to be used for the Static Conduction Test.

the vacuum tank test facility is capable in all respects of handling the flows and energies anticipated in these tests.

5.3.6 Preliminary Test Plan

Tests of the sub-scale disk generator will proceed in four steps: (1) Check-out of the resistojet heater, (2) unseeded hydrogen flow tests in the disk generator to verify the thermal design, (3) seeded flow tests to verify the operation of the seeding system and (4) power generation tests. The power generation tests will be aimed at exploring a matrix of operating conditions spanning the expected conditions in the full scale generator. The parameters to be varied include the stagnation temperature of the gas, the Mach number of the nozzle, the seed fraction, and the flow rate of hydrogen. Since the MHD interaction is not expected to be sufficient to fully utilize the stagnation pressure of 20 bars in the resistojet, it is expected that the flow will be supersonic throughout the disk. Therefore, the only requirement is that the exit back pressure within in the vacuum tank be less than the static pressure within the disk generator.

Given the fact that the MHD interaction is insufficient, it is likely that in some operating conditions the flow in the disk will separate. In these cases it may be desirable to go to lower pressures than 0.1 atmosphere back pressure in order to fill the disk generator. Table 14 provides a sample matrix of test conditions which should be explored.

Table 14. Typical Test Matrix

Test	T_o (K)	p_o (bar)	p_{tank} (bar)	Seed Mole %	M
1	2150	1	0.14	0.0015	1.7
2	2150	1	0.14	0.0050	1.7
3	2350	2.4	0.14	0.0015	2.4
4	2350	2.4	0.14	0.0050	2.4
5	2800	11	0.22	0.0015	3.1
6	2800	11	0.22	0.0050	3.1
7	2900	20	0.35	0.0015	3.2
8	2900	20	0.35	0.0050	3.2

CHAPTER 6

RECOMMENDATIONS FOR FURTHER WORK

6.1 Technical Objectives

The work reported and discussed in the preceding chapter has established the high performance potential of an MHD Disk Generator driven from a NERVA reactor can be realized with a stable plasma flow regime. The central objective of further work should accordingly be to demonstrate experimentally that the stable conduction mode can be attained in a small scale non-equilibrium disk MHD generator.

6.2 Technical Approach and Methodology

To achieve this objective, four complementary activities are proposed to take the project forward to a point where, at the conclusion of Phase II, the engineering basis will exist from a prototype system may be developed. These four activities are discussed in this Section, based on the results obtained in Phase I. They are identified as follows:

(1) Experimental Determination of Plasma Properties.
(2) Engineering Design.
(3) Test of Experimental Disk Generator.
(4) Engineering Evaluation.

6.2.1 Experimental Determination of Plasma Properties

The work undertaken in Phase I and reported in preceding Chapters 4 and 5, established that experiments should be set up at the beginning of Phase II to investigate plasma stability and to enable the limiting electrical strength of the disk insulator walls to be established. Several approaches will be taken in Phase II, one based on a static experiment along the lines of the original work by Kerrebrock and the second utilizing a shock tube facility. As will now be explained, the static experiment will also enable the limiting electrical strength to be studies. This will be implemented through the design and construction of a test rig in the laboratories of the STD Research Corporation while the disk studies will be performed by the Tokyo Institute of Technology, utilizing facilities located on its campuses at Nagatsuta and O-Okayama.

The Phase II approach to verification of plasma stability at the proposed operating conditions of the hydrogen-driven disk is to utilize a proven, flexible, well-diagnosed, experiment to pass current through realistically simulated working fluids never studied

experimentally before, under conditions of sufficient control and diagnostics to create an accurate map of the regimes of stable operation of the hydrogen-driven disk. A derivative benefit of these tests is that this facility also affords the opportunity to verify the breakdown strengths of pure hydrogen that may be used as a buffer on the insulator walls to prevent local concentrations of heat or electrical power.

Safety considerations preclude laboratory work with large volumes of pure hydrogen, but this is not necessary as the requisite data may be obtained using a noble gas-hydrogen mixture with seed. The candidate noble gases are argon and helium and information obtained by Shioda, Yamasaki and their associates for these gases are available (Ref. 8). Table 15 lists the basic Characteristics of the three facilities to be utilized. Two already in operation are located at Nagatsuta and the remaining one is under construction at O-Okayama and will be completed in April 1992. The third of these is the recently completed facility intended specifically to increase the thermal input for disk generator studies to 5 MW from the 2 MW available at Nagatsuta. Two experiments are proposed as follows: (1) determination of the inelastic energy loss factor for cesium-seeded argon or helium mixed with hydrogen; (2) studies of the effect of hydrogen addition on the performance of a cesium-seeded argon or helium plasma disk generator.

The determination of the inelastic energy loss factor will be carried out using the #1 Nagatsuta shock tube to drive a Faraday generator. The selection of a Faraday generator will be used as the measurement of Faraday current required in this work is exceedingly difficult to perform in the case of disk geometry. In contrast, current densities can readily be measured in a Faraday type generator and this will enable the inelastic loss factor to be determined from the electron energy equation through the measurement of current density, electron temperature, and electron number density using methods already established (Ref. 8) and in use by the Tokyo group.

Experimental studies using a shock tube have proved to be most valuable as a basis for both designing steady state non-equilibrium generators and also for gaining an understanding of the performance to be expected. For example, this technique has been used most successfully by a Tokyo group in preparing for the tests conducted using its Fuji-I blow down facility (Ref. 28). Again, because of safety considerations, the approach will be to add hydrogen, initially to the existing small scale shock tube driven disk generator (thermal input 1–1.5 MW) which is currently being operated on the #2 Nagatsuta facility. In determining the amount of hydrogen addition required, the work of Louis and Klepeis (Ref. 24) for an experiment involving nitrogen as a driver gas will be utilized as a guide, with the proviso that safety limitations on hydrogen are not exceeded. Based on the experience gained on this small-scale shock tube, the larger (thermal input = 5 MW with swirl and low seed fraction) will be used specifically to explore the stability of a cesium-seeded argon or helium plasma to which hydrogen has been added in a disk generator.

6.2.2 Engineering Design

The design, construction and operation of an experimental disk generator is the major activity proposed for Phase II. This will involve additional analysis based on the results of Phase I to refine the Reference Case, hardware and instrumentation design, fabrication and test. These aspects are now considered in turn.

The Phase I effort sequentially involved the determination of a Reference Case with the desired performance and subsequent verification that stable operation could be obtained. Review of this work indicates that some fine tuning of the "Reference Design" is needed. Application of the results presented in Figure 19 to the Reference Case shows this to be located too close to the hydrogen stability boundary to be acceptable as defined by Tables 4 and 5. The development of a "Modified Reference Case" will primarily involve a slight increase in seed faction to permit a reduction in electron temperature. The change of enthalpy extraction will be small and could, in fact, lead to a net increase due to the reduced electron Joule heating required. Other parameters will be adjusted as necessary to define the Modified Reference Case as closely as possible in parameters and performance to the corresponding Phase I Reference Case.

The Modified Reference Case for the full-scale system will then be applied to define the operating conditions of the subscale disk experiment. The design of the engineering test generator will also be guided by the results of the static conduction tests which will map the boundaries of stable conduction in the disk. The engineering aspects dealing with mechanical and thermal lifetimes will be partially addressed in the static conduction tests, because similar stresses and materials will be encountered in the smaller static tests. The modified Reference Case will serve as the basis of the final test plan for the experiment.

6.2.3 Test of Experimental Disk Generator

Once stable conduction is demonstrated and theoretical work can predict experiment, it still remains to make power with a real device. The proposed subscale experiments will prove that power generation is efficient and stable over the entire calculated operating envelope of the full scale generator. Preliminary calculations indicate that, because of hydrogen's very high specific enthalpy, it is likely that significant amount of energy extraction will be achieved. For example, if the enthalpy extraction is just a modest 5%, this will represent a specific energy extraction in excess of 2 MJ/kg, a world record for MHD power generation.

6.2.4 Engineering Evaluation

The data to be obtained from the analysis and experimental generator activities just discussed will enable the uncertainties identified at the outset of the Phase I effort to be removed and will permit an engineering evaluation to be conducted in sufficient detail to document the prototype development which will constitute Phase III of this project.

Two main lines of investigation will be pursued, one being the final selection of system operating conditions and the effect of these selections on system specific mass and the other the scaling and performance of the non-equilibrium MHD disk generator itself. With regard to system operating conditions, some revisiting of original assumptions is already indicated as a result of the Phase I work and undoubtedly will be further emphasized as Phase II progresses. Examples of this activity can only be cited. The actual analysis conducted will be determined primarily by the results of Phase II but also by mission requirements as perceived by SDIO, DOE and NASA at that time.

The Westinghouse Multi-Megawatt MHD Space Power Systems Study was used as a starting point for Phase I and the assumption that a modified NERVA reactor with a hydrogen exit temperature of 3000 K would be required as taken as an input. Examination of the Phase I results indicates that a reduction of this temperature to the tested NERVA value of 2550 K may not significantly reduce the system performance from an enthalpy extraction point of view. Further, the use of 1 atm as the generator exit pressure can certainly be relaxed somewhat in the space environment. Taking these two considerations together, some further systems analysis with the objective of determining the performance and dimensional changes resulting from reducing the reactor temperature and also dropping the exit pressure would be a useful line to pursue. The work will be done in sufficient detail to enable the effect on system specific mass to be established and so to provide a basis for trading off a presumable somewhat reduced performance and consequent increase of mass against the great advantage of using a reactor with fuel which operated successfully over 20 years ago.

A second area for investigation is likely to be output voltage which was established in the vicinity of 40 kV on the basis that this was the lowest value that could reasonably be allowed in combination with chopper-type direct DC-DC converters and a 100 kV busbar requirement. The investigation of the electrical strength of the disk insulator walls will establish limits which may not, in fact, allow this magnitude of voltage with the Modified Reference Case or, alternatively, require a considerably larger disk to accommodate this value. A fruitful area of analysis would, therefore, be to explore the consequences of the real voltage gradient limit. It may also be useful to determine what should be done to modify the generator if a DC busbar voltage lower than the 100 kV assumed in this study should be required. The intriguing prospect is that an application will emerge for which the disk generator can directly provide output voltage

with, at most, a switching type regulator to maintain the desired voltage level within specified limits.

For the MHD generator, a major objective will be to establish not only the scaling laws but also that no phenomena will occur in full-scale machines which, by virtue of stronger MHD interaction dependance cannot be expected to be observed in the small scale disk to be tested in Phase II. To the extent possible within the Phase II resources, 3-D generator codes developed on a proprietary basis by STD Research Corporation will be utilized to show how the data obtained in Phase II can be confidently applied to the design of larger MHD disk non-equilibrium generators.

Table 15. Japanese Shock Tube Facilities

Location	Nagatsuta #1	Nagatsuta #2	O-Okayama
1. Shock Tube			
h.p. section length, m	1.2	2.3-4.0	2.0-4.0
l.p. section length, m	8.8	8.5	8.0-12.0
inside diameter, mm	130	130	254
stagnation gas pressure, MPa	0.1-0.2	0.2-0.3	0.5
stagnation gas temperature, K	1900-2500	900-2500	1900-2500
2. Generator			
type	Faraday	Disk	Disk
inlet area, mm^2	26-70	--	--
outlet area, mm^2	60-70	--	--
inlet radius, mm	--	100	110
outlet radius, mm	--	360	280-300
channel height, mm	--	6-20	15-45
Thermal input, MW	--	2	5
magnetic field, T	--	2.6	3.0

For long operating time or steady state disk MHD generators, investigation of wall cooling will be required. The most attractive insulating wall material is aluminum oxide. Prior work at NASA LeRC by R. J. Sovie in a large non-equilibrium steady-state closed loop generator facility, demonstrated that construction of the generators insulating walls

of aluminum oxide brick backed by felt, for thermal insulation and expansion, provided a reliable design for operation up to wall temperatures of 2000 K, at least in the generator inlet region, some wall cooling must be provided in the generator inlet region. It may be possible to provide the required cooling by using less than 1% of the hydrogen flow to provide transpiration cooling. Tungsten should be good material for construction of the generator anode and cathode rings.

Cryogenic generator magnet construction will be considered using a conductor design similar to that developed by NASA LeRC for their 10–20 T neon cooled cryogenic magnets. This conductor holds the high purity aluminum in a structural channel to form a ribbon which with the addition of turn to turn insulating spacers can be wrapped into a magnet. For the subject system, magnet cooling would be provided by liquid hydrogen, which is a better coolant than neon, although more difficult to handle in the laboratory.

Additional aspects of the magnet design that require further study include selection of the desired field strength and its radial variation. The values selected for the Phase I study were only representative values. Also, of interest is the possibility of a single coil rather than a split pair coil magnet design. A concept suggested in a prior Westinghouse reported study in which most of the present HMJ Team members participated.

The importance of DC-DC convertors has already been emphasized. The design of these will be refined to take advantage of the latest switch and component technology available for the space environment. If compatible controlled switches become available, the further mass reduction obtainable by operating the entire power conditioning subsystem at liquid hydrogen temperature will be explored.

CHAPTER SEVEN

CONCLUDING COMMENTS

The pioneering proposal for the development of a prime mover capable of directly generating electricity through the expansion of an electrically conducting gas flowing in a magnetic field is generally credited to Karlovitz. To develop what was originally called an electromagnetic turbine and now is usually referred to as an MHD generator, Karlovitz realized that the electrons required to create a conducting fluid should be introduced by an auxiliary excitation scheme so that the electrical conductivity obtained would not be limited to that possible by thermal ionization alone. His method was to inject electrons into a combustion gas, a process which can now be appreciated would not succeed because of recombination in molecular gases. Towards the end of his investigations at the Westinghouse Research Laboratories in 1945-46, he resorted instead to seeding with potassium salt and accepted the electron density provided by thermal ionization. This approach has been taken by most MHD investigators and a very considerable amount of research and development data and experience have been gained on combustion driven MHD generators operating with potassium seed introduced into the combustion product flow.

The possibility of utilizing extra-thermal ionization remained an intriguing prospect, however, and Kerrebrock in 1960 first showed how the motionally induced electric field in an alkali metal vapor flow could lead to non-equilibrium hot electrons and accordingly enhance conductivity. This result was also obtained for cesium seeded noble gases, helium, argon and neon being the candidates, by investigators in a number of countries. The intent of this work was to operate the MHD generator from a high temperature nuclear reactor but the technology of commercial reactors of this type was never able to reach the required temperature ($\sim$2000K) without excessive fission product release from the fuel rods. For this reason, work on what came to be known as non-equilibrium MHD generators was largely abandoned although it was maintained by a few research groups, notably that of Louis at the Massachusetts Institute of Technology, Rietjens at the Eindhoven University of Technology and Shioda at the Tokyo Institute of Technology.

The extraction of sufficient enthalpy to make the MHD generator attractive has long been recognized as the central issue and the percentage extraction of the combustion driven equilibrium generators is limited by the temperature range over which adequate ionization is possible. For non-equilibrium generators, the ability to maintain a conductivity value for the MHD interaction over a substantial temperature range has been recognized as the key advantage from the point of view of satisfying this criterion but it was tacitly assumed that only noble gases could serve as working fluids in such systems. The recognition by Demetriades, and also by Klepeis and Louis, that hydrogen, though a molecular gas, behaved more akin to argon or neon that to nitrogen, opened up the intriguing possibility

of achieving the benefits of a non-equilibrium MHD generator with cesium seeded hydrogen. This is also the ideal working fluid for a truly high temperature gas cooled reactor, as was demonstrated in the NERVA program conducted 20 years ago.

An additional consideration for non-equilibrium MHD generators has been that ionization instabilities have limited performance in the several experimental investigations undertaken by research groups around the world. The establishment that these instabilities could be avoided through very low seed fractions with complete ionization enabled Shioda and his colleagues to demonstrate for the first time truly impressive performance with non-equilibrium MHD generators using cesium seeded helium and argon as the working fluid. They further showed that the disk geometry was markedly superior for non-equilibrium ionization as the Faraday current could be closed within the gas and did not require an electrode structure in the Faraday circuit.

It remained only to show that non-equilibrium ionization could be achieved in hydrogen on the same basis as had been demonstrated for noble gases. Professor Louis, to whom this report is dedicated, was most eager to undertake this work and surely would have but for his untimely death in 1988. As this report has discussed in detail, analytical steps to implement this goal have been taken by the HMJ team in Phase I. The outcome has been to achieve four major results which may be highlighted as follows:

1. A cesium seeded hydrogen disk MHD generator driven from a NERVA reactor heat source yields an overall specific mass of at least 15 MJ/kg and a specific dry mass of around 0.1 kg/kW. These value make the system exceedingly attractive for multi-megawatt space power systems and warrant further investigation to develop an engineering design basis supported by critical experimental data.

2. A stable fully ionized plasma operating regime compatible with the system parameters required for the performance quoted in (1) above exists for hydrogen, corresponding to the argon and helium results reported by Shioda and his colleagues.

3. Critical parameters for plasma characterization can be determined experimentally using (a) a small scale static rig; (b) a small scale hydrogen disk generator, and (c) a hydrogen noble gas mixture in a shock tube. Candidate gases for point (c) are argon and helium.

4. A major improvement in the system mass can be achieved by utilizing direct DC-DC converters as a result of the high voltage disk generator voltage output.

The next part of this project must be largely experimental in character although, as the previous Chapter has indicated, some further system studies are required to optimize

system operating conditions. The static conduction and insulating wall demonstration experiment and the test of the sub-scale disk generator can be undertaken in the laboratory of the STD Research Corporation. The results of these experiments, together with shock tube disk generator work using hydrogen/noble gas mixtures at the Tokyo Institute of Technology will provide the engineering data necessary to design what may be described as the ultimate high performance electromagnetic turbine. The potential of this generator for multi-megawatt space applications has already been indicated in Chapter 2 and in due course it will also contribute to the development of advanced nuclear- electric systems for terrestrial use.

REFERENCES

1. R. R. Holman, "A Critique of NERVA-Based Nuclear Reactor Design and Performance for MMW Space Propulsion Applications," *Proc., Fourth Symposium on Space Nuclear Power Systems,* Albuquerque, N.M., 12-16 January 1987.

2. L. E. VanBibber, et al., "Conceptual Design of a Space Based Multi-Megawatt MHD Power System," Report W-AESD-TR-88-0002 (2 Vols.). Prepared for DOE by Westinghouse Corp., Pittsburgh, PA, January, 1988.

3. J. F. Louis and R. R. Holman, "A Nuclear Powered Space Based Disk MHD Power System Description and Performance Assessment," *Proc., 26th Symposium on Engineering Aspects of MHD,* Nashville, TN, June 1988.

4. C. D. Maxwell and S. T. Demetriades, "Feasibility Assessment for Space-Based Multi-Megawatt MHD Power Systems," Report, STDR-87-9 (2 Vols.). Prepared for DOE by STD Research Corp., Arcadia, CA, Feb. 1988.

5. A. Solbes, H. Iwata, "Multimegawatt Disk Generator System for Space Applications," *Proc., 28th Symposium on Engineering Aspects of MHD,* Nashville, TN, June 1988.

6. D. W. Swallom, et al., "Multimegawatt Combustion-Driven Magnetohydrodynamics Power Systems," *Proc., 28th Symposium on Engineering Aspects of MHD,* Nashville, TN, June 1988.

7. A. Veefkied, "Inert Gas MHD Generator Experiments with a Stock Tunnel Facility," *Magnetohydrodynamics International Journal,* 2, pp. 149-162, 1989.

8. N. Harada, et al, "High Enthalpy Extraction Demonstration with Closed Cycle MHD Disk Generators," *Proc., 28th Symposium on Engineering Aspects of MHD,* Chicago, IL, June 1990.

9. F. B. Bernerd, et al, "High Voltage, Nonequilibrium MHD Disk Generators," *Proc., 10th International Conference MHD Electrical Power Generation,* Vol. III, p. XII.64, Tiruchchirappalli, India, December 1989.

10. R. J. Rosa, "Magnetohydrodynamic Energy Conversion," *McGraw Hill Book Co.*, New York, NY, 1968.

11. P. Wood, "Switching Power Converters," *Robert E. Krieger Publishing Company,* Malibar, FL, 1984.

12. W. D. Jackson and P. Wood, "Power Conditioning for Multi-Megawatt Space Electric Systems," Report HMJ-88-1115 prepared for DOE by HMJ Corp., Chevy Chase, MD, Dec. 1988.

13. S. T. Demetriades, "Determination of Energy Loss Factors for Slow Electrons in Hot Gases," *Phys. Review,* 158, pp. 215–217 and U. S. Dept. of Commerce/NBS Reports N69-35413 (August 1968) and N70-15044 (August 1969).

14. G. W. Sutton and A Sherman, *Engineering Magnetohydrodynamics,* McGraw-Hill, 1965.

15. E. W. McDaniel, *Collision Phenomena in Ionized Gases,* John Wiley & Sons, New York, 1964.

16. S. T. Demetriades, C. D. Maxwell, and D. A. Oliver, "Progress in Analytical Modeling of MHD Power Generators, II," *Proc., 21st Symposium on Engineering Aspects of Magnetohydrodynamics,* Argonne National Laboratory, Argonne, Illinois, June 1983.

17. S. T. Demetriades, J. T. Demetriades, and A. S. Demetriades, "Influence of Magnetic Reynolds Number on Power Generated by an Ideal MHD Device," *AIAA Journal,* 1985.

18. S. T. Demetriades and G. S. Argyropoulos, "Ohm's Law in Multicomponent Nonisothermal Plasmas with Temperature and Pressure Gradients," *Phys. Fluids,* Vol. 11, No. 12, pp. 2559–2566.

19. G. S. Argyropoulos and S. T. Demetriades, "Influence of Relaxation Effects in Nonequilibrium J × B Devices," *J. Applied Physics,* Vol. 40, No. 11, pp. 4400–4409.

20. E. P. Velikhov, "Hall Instability of Current-Carrying Slightly Ionized Plasmas," *Proc., Symposium on MHD Power Generation,* Newcastle-upon-Tyne, 1962.

21. J. L. Kerrebrock, "Nonequilibrium Ionization Due to Electron Heating: I. Theory and II. Experiments," *AIAA Journal,* Vol. 2, No. 6, June 1964.

22. E. P. Velikhov and A. M. Dykhne, "Plasma Turbulence Due to the Ionization Instability in a Strong Magnetic Field," *Proc., 6th International Conference on Ionization Phenomena in Gases,* Vol. 4, pp. 511–512, Paris, 1963.

23. A. Solbes, "Quasi Linear Plane Wave Study of Electrothermal Instabilities," *Proc., Electricity from MHD,* Warsaw, Paper SM-107/26, 1968.

24. J. E. Klepeis and J. F. Louis, "High Hall Coefficient Studies in a Disk Generator Driven by Molecular Gases," *Proc., 10th Symposium on Engineering Aspects of MHD,* pp. 202–204, 1968.

25. J. E. Klepeis and J. F. Louis, "Studies with a Disk Generator driven by Molecular Gases," *Proc., 11th Symposium on Engineering Aspects of MHD,* Pasadena, CA, pp. 62–63, 1970.

26. G. S. Argyropoulos, S. T. Demetriades, and A. P. Kendig, "Current Distribution in Nonequilibrium J × B Devices," *J. Applied Physics,* Vol. 38, pp. 5233–5239 (1967).

27. C. D. Maxwell, J. T. Demetriades, D. A. Oliver, and S. T. Demetriades, "Consideration of Optimal Boundary Configurations for Linear MHD Generators," *Proc., 22nd Symposium on Engineering Aspects of Magnetohydrodynamics,* 26–28 June 1984, MHD Energy Center, Mississippi State University, Starkville, MS, pp. 2:1:1 to 2:1:25.

28. H. Yamasaki, eet al.,, "High Enthalpy Extraction in the FUJI-1 disk Generator Experiments," *Proc., 10th Int. Conf. MHD Elec. Pwr Gen.,* Vol. III, P. XII.3, Tiruchirapalli, India, December 1989.